ADSORPTION OF MODEL MICROPOLLUTANTS TO POLYMER FILMS AFTER UV LIGHT EXPOSURE

A Thesis

SUBMITTED TO THE FACULTY OF THE UNIVERSITY OF MINNESOTA

BY

Faith E. Murphy

IN PARTIAL FULFILLMENT OF THE REQUIREMENTS

FOR THR DEGREE OF

MASTER OF SCIENCE

Dr. Melissa A. Maurer-Jones

July 2019

Acknowledgements

I would like to acknowledge the University of Minnesota Duluth, specifically the Swenson College of Science and Engineering and the Department of Chemistry and Biochemistry, for providing research opportunities and financial support. I would also like to acknowledge financial support from the Minnesota Chromatograph Forum.

I would like to thank faculty members Dr. Jacob Wainman and Dr. Kathryn Schreiner for their encouragement and support throughout this project. They always seemed to be there when I needed it the most and for that, I am very grateful.

I would also like to thank the MMJ lab group, specifically Daniel Zoltek and Raven Buckman for helping me with data collection. I cannot express how important you all were with keeping my sanity over the past few years. I am so thankful to have shared many deep talks and the biggest belly laughs with you. You were always supportive, kept my head on straight, and most importantly, let me vent when I needed to. I wish you all the best in your future endeavors.

I would especially like to thank my thesis advisor Dr. Melissa A. Maurer-Jones. It is hard to know where to begin expressing gratitude for all the help she has provided me since I began researching with her. She not only taught me how to become a successful chemist, but I learned a lot about myself during my time researching under her. I am extremely thankful for her mentorship and guidance when this project got tough. I also cannot stress how thankful I am for your patience and kindness when I struggled with both life and research. She amazingly knew when I needed compassion, or when I needed a kick in the pants. I have learned so much from her and I hope I can have a large positive impact on someone else just like she did to me.

Dedication

To my dad, who is forever proud and never stopped believing in me.

Abstract

Plastics have proven to be useful in a myriad of applications due to properties like chemical resistance. However, this also makes them a problematic, persistent environmental contaminant. In the environment, plastics are known to degrade from environmental factors including UV light irradiation. Previous studies have shown that plastics have an ability to sorb organic compounds, causing plastics to act as vectors for contaminant transport through the environment that ultimately causes accumulation within various aquatic organisms. Yet, little work has evaluated if plastic weathering impacts its behavior in the environment. This work aims to quantify sorption of coumarin, a model pollutant molecule, onto photodegraded polymers. The main polymers studied for this work are polyethylene (PE) and polyethylene terephthalate (PET) since they are abundantly found as waste in marine environments. Photo-transformations of polymer films were characterized by ATR-FTIR and SEM after irradiation with 254 nm UV light to understand molecular and structural changes. Coumarin adsorption to non-photolyzed and photolyzed plastic films were evaluated with liquid chromatography (UPLC) and the monitored data was fit to the Freundlich and Langmuir sorption isotherms to quantify pollutant partitioning. Correlations between distribution coefficients and plastic phototransformations affecting hydrophobicity and crystallinity were analyzed. The distribution coefficient of coumarin was higher for 0 h UV PET than PE. For both types of plastic, distribution coefficients of coumarin initially decreased then increased from either 24- or 48- time points. The trend for the distribution coefficient therefore cannot be only related to changes in polymer hydrophobicity and crystallinity. This work has contributed to a better understanding of the interaction between plastic debris and organic pollutants found in water.

TABLE OF CONTENTS

LIST OF TABLES

LIST OF FIGURES

LIST OF ABBREVIATIONS

PE	Polyethylene
PP	Polypropylene
PVC	Polyvinyl chloride
PET	Polyethylene terephthalate
MP	Microplastic
WWTP	Waste water treatment plant
HDPE	High density polyethylene
LDPE	Low density polyethylene
PCB	Polychlorinated biphenyl
PAH	Polyaromatic hydrocarbon
UV	Ultra-violet
XLPE/PEX	Crosslinked polyethylene
UPLC	Ultra-high performance liquid chromatography
CI	Carbonyl Index
FTIR	Fourier transform infrared spectroscopy
ATR	Attenuated total reflectance
SEM	Scanning electron microscopy
XRD	X-ray diffraction
AFM	Atomic force microscopy
DSC	Differential scanning calorimetry

LIST OF SYMBOLS

K_f	Freundlich constant or capacity factor
n	Freundlich exponent
C_{solid}	Concentration adsorbed on solid phase
C_{water}	Concentration in aqueous phase
$C_{solid,max}$	Maximum concentration that can adsorb on solid
K_d	Distribution coefficient
$C_{solid,max}$	Amount of adsorbed molecules for monolayer coverage
K_{ow}	Octanol-water partitioning coefficient
$A_{carbonyl}$	Area under FTIR carbonyl band
$A_{normalization}$	Area under FTIR normalization band
X	Percent crystallinity for PE
I_{cr}	Area under crystalline FTIR band
I_{am}	Area under amorphous FTIR band

CHAPTER 1: INTRODUCTION

1.1 Presence of Plastics in Natural Systems

Plastics have proven to be useful in a myriad of applications because of their ability to be modified for a variety of functions that has led to mass production. It has been estimated that about 8.3 billion metric tons of plastics have been produced to date[1] and in 2012 it was projected that 48 million tons were being produced each year.[2] The most commonly produced are polyethylene (PE, 36%), polypropylene (PP, 12%), polyvinyl chloride (PVC, 12%), and polyethylene terephthalate (PET, <10%).[1] The majority of these plastic products are disposed of after a single use.[1] It is becoming clear that the reasons plastics are so widely used, which include durability and inexpensiveness, are causing harm to the environment. The longevity of plastic causes them to accumulate on land, in water, and in sediments.[3-5] Of all the plastic ever made, it is estimated that 60% has made its way to the sea.[1] Plastic can enter marine environments from poorly managed landfills, runoff from vastly populated coastal cities, fishing, and shipping. Plastic pollution can also be from illegal or intentional dumping, both by consumers and industries.[6] Once these plastics make it into our environment, they can exist for hundreds to thousands of years,[7] and are dispersed over long distances due to their buoyancy.[8] Although plastics have the ability to travel far distances, the world's oceans have natural water currents that create gyres where plastic debris converges. The discovery of vast plastic accumulation in the five gyres, colloquially given the term 'garbage patches,' made oceanic pollution very apparent. It is estimated plastic levels in the North Pacific Garbage Patch are at 335,000 plastic items per square kilometer.[9]

Of the plastics floating around, one concerning form are microplastics (MP), which are defined as plastic particles that are less than five millimeters in size. [10] Plastic debris does

not always stay in its initial form as there are mechanical and chemical processes that cause degradation. The classification for MP that come from larger plastic breakdown is secondary MP, where as a primary MP is an intentionally manufactured micro-sized particle. It is estimated of all the plastic particles floating at sea, 5.25 trillion are secondary MP.[11]

A main source of MP in the environment besides degradation is effluent from wastewater treatment plants (WWTP). It is estimated that 8 trillion microplastic particles are emitted from WWTP per day in the United States,[12] and come from sources such as clothing fibers after washing or personal care products containing microbeads. Industrial plants have also been deemed a source of MP.[13] Plastics are present in all major ocean environments[10] as well as in freshwater ecosystems.[14,15] Dris et al. reviewed multiple studies showing that not only are microplastics present in freshwater systems, but contamination levels in freshwater is similar to that of oceans, relative to volume.[16]

1.2 Implications of Plastic Pollution

Plastic pollution's presence and persistence has many negative effects on ecosystems. Public concern has often centered around entanglement and plastic ingestion, and the impacts of these problems have been well documented across trophic levels.[17-20] Overall, more than 250 different species have been found to be affected by plastic ingestion.[21] Figure 1.1 shows plastic accumulation in zooplankton, studied by Cole et al.[22]

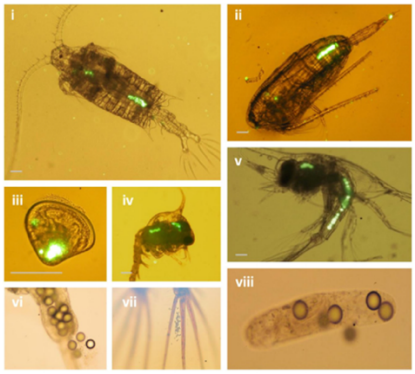

Figure 1.1: Microplastics of different sizes can be ingested, egested and adhere to a range of zooplankton, as visualized using fluorescence microscopy: (i) the copepod Centropages typicus ii) the copepod Calanus helgolandicus (iii) a D-stage bivalve larvae (iv) a Brachyuran (decapod) larvae (zoea stage) (v) a Porcellanid (decapod) larvae (vi) copepod Temora longicornis (vii) C. typicus; (viii) a T. longicornis faecal pellet.[22]

Many researchers have also studied the effects of plastic ingestion on higher tropic levels.[23] For example, Moser and Lee found that 55% of reported seabird species are affected by plastic ingestion,[24] even Antarctic seabirds that are away from highly inhabited regions.[25] The negative effects of plastic ingestion include but are not limited to decreased feeding, decreased hormone levels, reproductive issues, and gastrointestinal blockages.[26] Unfortunately, plastic pollution may be greatly underestimated as most victims are likely to go undiscovered over oceans, as they either sink or are eaten by predators.[27]

1.3 Sorption Capabilities of Polymers

1.3.1 Polymer Sorption and its Implications

While ingestion and entanglement pose important concerns for ecosystem health, plastics in the environment can also sorb other chemical and biochemical molecules that result in plastics acting as vectors for contaminants. Many studies have shown that polymers have the ability to sorb organic compounds.[28-30] Commonly sorbed organic contaminants consist of polychlorinated biphenyls (PCBs), polycyclic aromatic hydrocarbons (PAHs), and many more.[31-33] Plastics often act as a sink for organic compounds and lower the aqueous concentration of said contaminants. On the contrary, if the these molecules are non-covalently bound, previously sorbed contaminants can be desorbed if the surrounding environment changes.[34,35] Furthermore, plastics have been found to leach additives, some of which are known toxicants.[36] This complex relationship between plastics and environmental contaminants has been studied frequently in recent years.[17,31-33,37-41] In a study by Chen, 84% of the plastics sampled in the North Pacific Garbage Patch had at least one sorbed chemical that exceeded its environmental concentration standard.[42] Studies on sorption have also shown plastics like high density PE (HDPE), low density PE (LDPE), and PP sorb ten times

higher of concentrations of organic pollutants than PET and PVC.[28] Because of plastics' ability to both sorb and leach chemicals, researchers have deemed them a medium for transporting pollutants throughout marine environments.[17,39]

Previous research supports the idea that since polymers have the ability to transport contaminants, there is a possibility of bioaccumulation.[38] Figure 1.2 visually represents the many pathways and interactions that occur between plastics and contaminants.

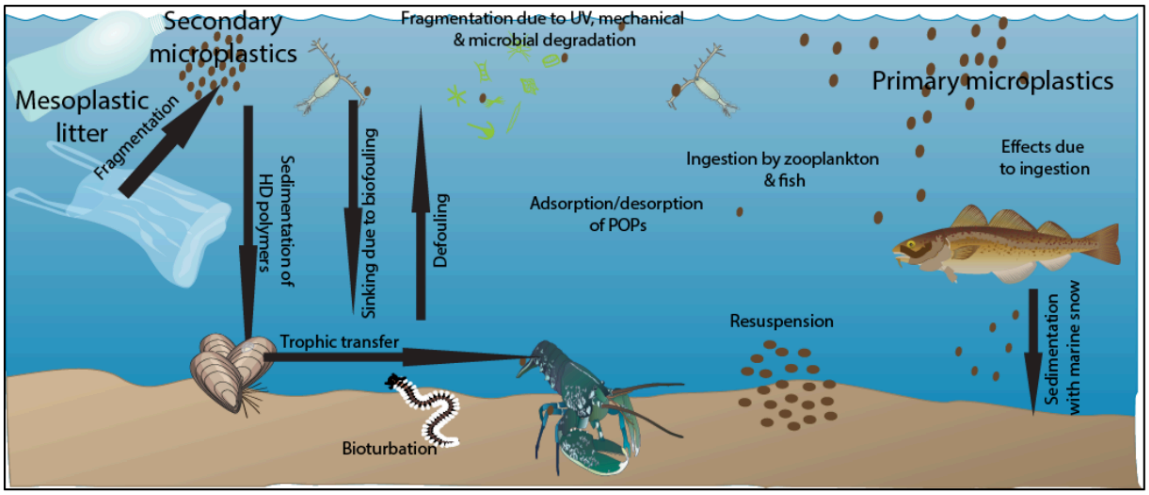

Figure 1.2: Potential fate, pathways and biological interactions of plastics and pollutants.[20]

One problem with MP ingestion after contaminant sorption begins with MP's ability to remain in organism's systems for long periods of time. A study by Browne et al. showed mussels fed microplastics had the particles enter in their circulatory system within three days where they remained for more than 48 days.[18] Many studies have even shown that organisms ranging from worms to seabirds have accumulated organic chemicals from ingested plastics.[17,38,43] In a study by Rochman et al., fish were fed plastics that had sorbed a variety of organic pollutants that accumulated in the fish tissue, causing hepatic stress.[44] Similar studies where organisms were fed plastics containing harmful chemicals resulted in a variety of problems like altered gene expression and reduced population growth.[43,45] The possibility

of biomagnification means human health is also at risk because the commonly sorbed contaminants have been linked to different human health problems like endocrine disruption, cancer, neurobehavioral changes, diabetes, and more.[46-49]

Although the implications of polymer sorption are becoming more widely studied, there are many gaps in knowledge on the fate of polymer sorption that have not been studied yet. For example, photodegradation of polymers by sunlight significantly changes the molecules of the polymer, but its effects on polymer-pollutant adsorption is not well understood. This thesis seeks to address this critical gap in understanding the behavior of polymers in our aqueous systems.

1.3.2 Quantifying Adsorption with Isotherms

In order to quantitatively study the effects of polymer photodegradation on sorption, sorption isotherms are applied to experimental data to give rise to distribution coefficients for the type of plastics used in this study. The name for solutes that undergo sorption are commonly termed sorbates whereas the sorbing phase is called the sorbent. There are two broad classes of sorption that exist, adsorption and absorption. In adsorption, accumulation of the sorbate is generally limited to a surface/interface between the solution and sorbent. However, in absorption, the sorbent is transported between the phases and penetrates the sorbent phase by at least several nanometers. For a molecule to be absorbed, it would need sufficient energy to overcome attractive forces between polymer chains.[50] It is assumed in polymer sorption experiments that adsorption is the main process occurring. This is supported by the multitude of research that shows low and slow vapor permeability and diffusion of small molecules.[51,52] These results from previous experiments suggest that large,

non-volatile molecules would not readily diffuse, therefore, adsorption is the only occurring polymer-pollutant interaction.

Adsorption can be classified in three subclasses: physical, chemical, and electrostatic. Focusing on physical adsorption, these relatively weak, non-covalent bonding forces become amplified in the case of hydrophobic molecules. A dissolved, non-polar molecule is held in aqueous solution by an ice-like arrangement of water molecules. The favorable enthalpy of this arrangement is countered by the unfavorable enthalpy resulting from the increased ordering of solvent molecules. This can result in solute molecules being driven from solution at concentrations below the maximum solubility if the system is thermodynamically favorable to adsorption. This combined effect of physical and dispersion-type interactions is often referred to as "hydrophobic bonding".[53] The medium of which adsorption is occurring changes the strength of hydrophobic bonding and therefore the amount of solute driven out of aqueous solution.

Organic contaminant sorption to polymers is typically quantified by equilibrium solid-water distribution coefficients, K_d, defined as (Eq. 1)

$$K_d = \frac{C_{solid}}{C_{water}} \quad (1)$$

where C_{solid} is the concentration of the compound on the solid phase and C_{water} is the concentration of the water phase at equilibrium.[54,55] These distribution coefficients are a quantitative measure of the free energy interaction for the contaminant and plastic, which largely direct the fate of organic contaminants in aquatic environments. Once known, distribution coefficients can be used to better predict the role plastics and MP play as contaminant-transporters.

Models used to characterize the equilibrium distribution of a sorbent between phases/interfaces typically relate the amount of solute sorbed per amount of sorbent, C_{solid}, to the equilibrium concentration in the solvent phase, C_{water}. This type of expression when evaluated at constant temperature is called a sorption "isotherm". Numerous conceptual and empirical models exist to describe adsorption patterns. One of the most widely used isotherm is the Simple Freundlich model.[56,57] It is based on the following relationship (Eq. 2)

$$C_{solid} = K_f C_{water}{}^{n} \quad (2)$$

where K_f (L g^{-1}) is the Freundlich constant or capacity factor and n is the Freundlich exponent. The linearized form has the equation (Eq. 3)

$$\log (C_{solid}) = \log(K_f) + nC_{water} \quad (3)$$

The Freundlich isotherm is strictly empirically determined. The model operates with the assumption that no maximum adsorption amount is reached and that each site exhibits a different sorption free energy.[58] Its application also becomes limited because it fails under high pressure and does not hold up when applied to high concentrations. If experimental data does not fit well with the Freundlich model, the assumptions behind this method may not be valid and other models should be applied to find a more appropriate model.

Another commonly used model is the Langmuir isotherm. The Langmuir model is based on the idea that there is a continuous chain polymer matrix with "microvoids" or holes frozen into the matrix.[59] The three main assumptions of this isotherm are that all adsorption sites: (i) are assumed to be identical, (ii) each site retains only one molecule of the given compound, and (iii) all sites are energetically and sterically independent of the adsorbed quantity.[60] This model also assumes there is a limited adsorption quantity, $C_{solid,max}$. Its equation is as follows: (Eq. 4)

$$C_{solid} = \frac{C_{solid,max} K_d C_{water}}{1 + K_d C_{water}} \quad (4)$$

where $C_{solid,max}$ is the amount of adsorbed molecules it takes for complete monolayer coverage. This equation linearized is as follows:

$$\frac{1}{C_{solid}} = \frac{1}{C_{solid,max}} + \frac{1}{K_d C_{solid,max}} \frac{1}{C_{water}} \quad (5)$$

Both the Langmuir and Freundlich models were applied on the experimental data and evaluated to determine which one best modeled the sorption data.

1.4 Photochemical Changes of Polymers

It is important to study polymers' photochemical changes that occur in the polymer molecule due to photodegradation to understand their influence on material properties and therefore, adsorption. Although the photodegradation of polymers has been widely studied, the impact of polymer photo-transformations on adsorption of contaminants is not reported. While the exact photo-chemical reactions are not the same between different polymer molecules, most polymer photo-transformations follow similar pathways of degradation. The three main and well researched mechanisms of polymer photodegradation are oxidation, scission, and crosslinking. These are discussed below, with detail paid to the polymers PE and PET, the primary polymers under study in this thesis (Fig. 1.3).

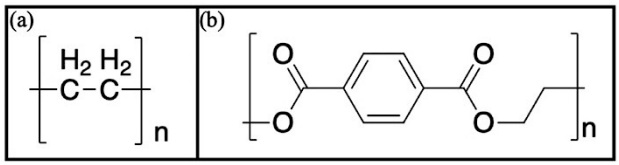

Figure 1.3: Structures of (a) PE and (b) PET.

1.4.1 Oxidation

In the presence of oxygen, oxidation is one of the first observed mechanisms during polymer photodegradation. This is due to the fast rate at which polymers oxidize. However, the yield of oxidation is not necessarily high. Oxidation causes physical and chemical changes to plastics, like yellowing, that ultimately affects the polymer's performance.[61] In polyolefins like polyethylene, primary photoproducts like hydroperoxides are formed when the plastics react with oxygen from the air. These hydroperoxides decompose through scission of the O-O bond,[62] which leads to alkoxyl and hydroxyl radical formation that are key intermediates to produce ketones. The ketones can further react photochemically by Norrish type I and type II reactions. The Norrish type I reaction consists of an alpha-cleavage reaction involving a triplet state formed in the carbonyl bond whereas the Norrish type II reaction consists of a hydrogen abstraction that can also lead to cleavage. Figure 1.4 shows the possible products from a Norrish type I reaction while Figure 1.5 shows the results from Norrish type II reactions.

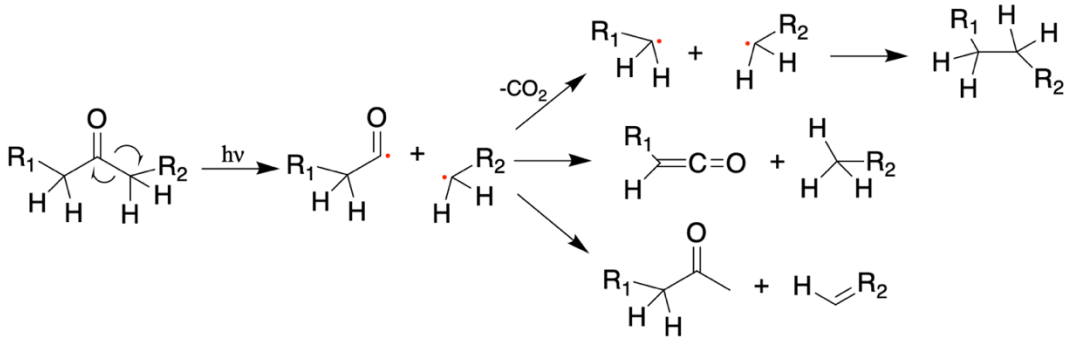

Figure 1.4: Schema for Norrish type I reactions.

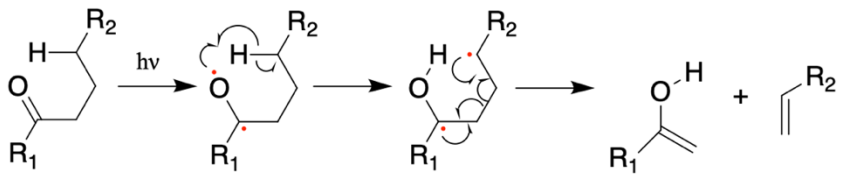

Figure 1.5: Scheme for a Norrish type II reaction.

In addition to the fast rates of this degradation pathway, oxidation is important to follow for this sorption experiment because of its effects on polymer hydrophobicity. Hydrophobic materials, such as PE, lack active groups on their surface that could hydrogen bond with water.[63] The formation of moieties like carbonyls, hydroxyls, and carboxylic end groups on the polymer surface causes more hydrophilic character.[64,65] Therefore, if oxidation via photodegradation creates these hydrophilic groups, the polymer's hydrophobicity changes, which in turn could affect the polymer's sorption capability with hydrophobic contaminants. Figure 1.6 shows the hypothesized oxidation mechanisms for PET that includes photodegradation products such as carboxylic acid groups and mono or dihydroxy terephthalate compounds.

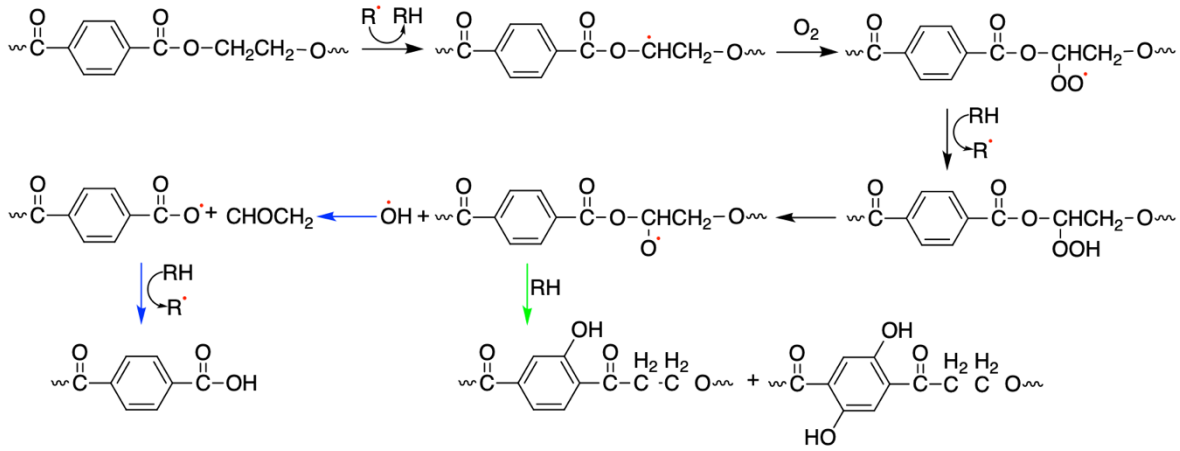

Figure 1.6: Schema and phototransformation products oxidation of PET via UV light.

1.4.2 Scission

Scission is the process of backbone cleavage in polymers, which commonly occurs for polymers such as PE, PP, and PET during degradation.[66,67] The scission process begins similarly to oxidation where a radical alkyl on the backbone is oxygenated, resulting in a hydroperoxide species. The hydroperoxide O-O bond will be cleaved to form an oxygen

radical and follow either Norrish type I or type II pathway.[68] PET can also undergo scission reactions via Norrish mechanisms, though it does not need oxygen from the air because the polymer backbone already contains an ester linkage.[69] Breaking of the polymer backbone leads to the formation of smaller polymer fragments that can leach out of the polymer matrix in the form of oligomers or larger MP fragments. Also, chain scission has been thought to lead to rearrangement of polymer fragments that ultimately increases crystallinity; this process has been termed chemi-crystallization.[70-72] Crystallinity is an important factor to consider for sorption mechanisms as previous studies have shown the ability for a chemical to diffuse through a polymeric material decreases with increasing crystallinity.[73] Specifically for PE, previous research has even shown sorption coefficients with water decrease with increasing crystallinity.[74] Therefore, changes in crystallinity as the result of polymer photodegradation could have key implications for pollutant sorption.

1.4.3 Crosslinking

Photoinitiated crosslinking has been majorly developed with the research involving chemical or electron-beam crosslinked polymers from a materials design perspective. For example, crosslinked-polyethylene (XLPE or PEX) is used in many infrastructure applications. However, crosslinking in polymers in the environment changes the mechanical properties of the plastics, often making them rigid and sometimes brittle. For most of the common plastics (PE, PP, PET, PVC), crosslinking is the outcome of radical recombination. UV-light induced photochemical crosslinking of polymers is not typically considered a primary path of photodegradation under ambient temperature conditions and O_2 present. This is because photo-oxidation degradation pathways dominate. Conversely, under a vacuum crosslinking becomes predominant.[75-77] Crosslinking is important to consider as previous

literature proposes the increase of crosslinking decreases crystallinity.[78,79] This decrease is attributed to the fact the crosslinking happens in the amorphous regions and therefore stabilizes the unwound state and disrupts packing.[80] The proposed crosslinking mechanisms and structures for PE and PET can be seen in Figures 1.7 and 1.8, respectively.

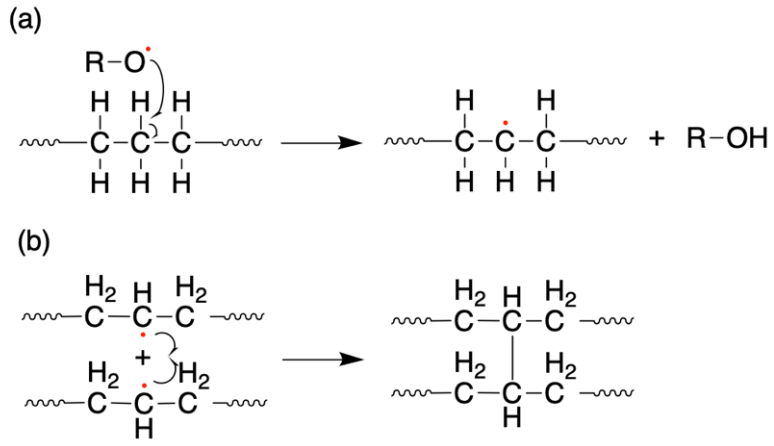

Figure 1.7: (a) Formation of PE alkane chain radical. (b) recombination of two PE chains to form crosslinked structure.

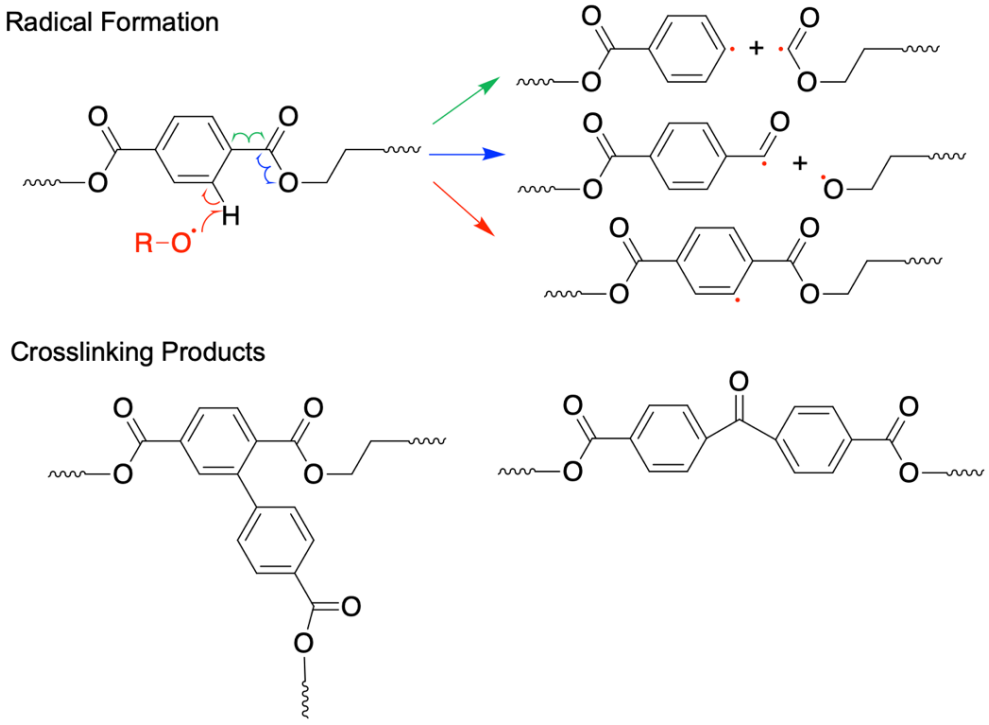

Figure 1.8: Schema for PET radical structures formed from photodegradation and recombination products.

1.5 The Need for a Better Understanding of Polymer Fate

With the dramatic increase of plastic pollution, the need for a better understanding of polymer-pollutant relationships also increases. Although the implications of polymer sorption are increasingly becoming studied, very little work has addressed the impact of photochemical transformations on pollutant-polymer distribution.

This hole has led to the aims for my research being two-fold:

1. To determine distribution coefficients for a coumarin and multiple polymer combinations, including both irradiated and pristine plastics.
2. To correlate coumarin adsorption and polymer photo-transformations.

It is important to characterize the photo-transformations of the polymers to get a better understanding of the changes to polymer hydrophobicity and crystallization, then relate these changes to polymer sorption capabilities.

The polymers used in this study were PE and PET as they are two of the most abundant types of plastic found in marine environments.[28,81] Coumarin was chosen as the model micropollutant in this study as it was the only non-volatile, hydrophobic chemical that was able to be studied using ultra-performance liquid chromatography (UPLC) with an equilibrium time of less than a month (see Appendix for other molecules tried). A common way to rank hydrophobicities of chemicals is using their octanol-water partitioning coefficients, K_{ow}. Coumarin properties are listed in Table 1.1 and its structure can be seen in Figure 1.8 below.

Table 1.1. Chemical and Physical properties of Coumarin.

Molecular Weight	**Log K_{ow}**	**Water Solubility**	**Vapor Pressure**
146.14 g mol^{-1}	1.39	1.7 x 10^{-3} g mL^{-1}	9.8 x 10^{-4} mmHg

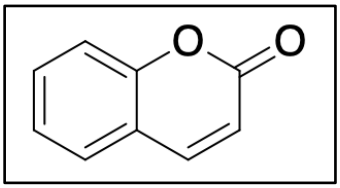

Figure 1.9: Structure of the experimental model micropollutant, coumarin.

CHAPTER 2

CHAPTER 2.1: MATERIALS AND METHODS

2.1.1 Chemicals and Sorbents

Coumarin was purchased from Acros Organics (Geel, Belgium). Acetonitrile (HPLC grade) was purchased from Fisher Chemical (Hampton, New Hampshire). Ultrapure water was taken from a Millipore Milli-Q Reference water purification system with an 18MΩ resistivity (Darmstadt, Germany).

Low density PE (LDPE), herein referred to as PE, and PET films were purchased from Goodfellow Cambridge Unlimited (Huntingdon, England) and used as sorbents. The film thicknesses reported in the data sheets were 0.03 mm and 0.025 mm for LDPE and PET, respectively. Thin films of PET and PE were presoaked in solvent for 24 hours each starting with hexanes, then methanol, and finally ultrapure water to pre-leach any processing additives or un-polymerized oligomers from the plastic films. The presoaked films were then mounted on cardstock and irradiated for 24, 48, or 72 hours on both sides, using a Rayonet Merry-Go-Round photoreactor (Southern New England Ultraviolet Corp, Bamford, CT). The reactor was equipped with 16, 254 nm light bulbs. This wavelength of UV light was chosen because it causes phototransformations of the polymers quicker than longer wavelengths, though the phototransformations products are the same.

2.1.2 Polymer Analysis

2.1.2.1 Hydrophobicity

PE's apparent hydrophobicity was characterized using the carbonyl index (CI). The CI was used to quantify oxidation of the samples using the attenuated total reflectance-Fourier transform infrared (ATR-FTIR) spectrometer. Infrared spectra were acquired using a Nicolet iS10 FTIR spectrometer (Thermo Scientific, Waltham, Massachusetts) that had a diamond crystal ATR attachment. All spectra were collected using OMNIC software with the following settings: scanning range of 600-4000 cm^{-1}, resolution of 4 cm^{-1}, and 64 scans. Each scan had a background taken immediately before, as well as each sample was scanned in triplicate on the front and back side of the film.

The CI was calculated was by measuring the area of the carbonyl band (around 1720 cm^{-1}) after baseline subtraction, then normalizing it to the area of the normalization band. For PE, the normalization band is the CH_2 wagging and CH_3 bending band (~1370-1380 cm^{-1}). Normalization accounts for variability in the amount of polymer on the ATR crystal. Therefore, the equation used for CI is shown in below (Eq. 5)

$$CI = \frac{A_{carbonyl}}{A_{normalization}} \quad (5)$$

where $A_{carbonyl}$ is the area of the carbonyl band (~1720 cm^{-1}) and $A_{normalization}$ is the area of the normalization band.

PET's apparent hydrophobicity was characterized using ATR-FTIR and fluorescence spectroscopy. Unlike PE, the FTIR spectra was used to qualitatively assess structural changes because the ester linkages make using CI irrelevant.

Fluorescence spectroscopy was used to measure the monohydroxylated species that are created from UV degradation of PET known to fluorescence at 460 nm. The

monohydroxylated species emission content for all PET samples was measured on a Horiba Fluoromax-4 spectro-fluorometer (Irvine, CA, USA) with a 1 nm slit width for both the entrance and exit slit. Solid samples were placed at a 45-degree angle from excitation and emission slits and the samples were excited at 340 nm with emission spectra collected from 360 nm to 600 nm.

2.1.2.2 Crystallinity

Previous studies have shown a doublet band due to the terminal carbon deformation that lies in the region between 1472 - 1456 cm^{-1} can be used to determine polyethylene crystallinity.[82,83] In this method, the orthorhombic (crystalline) band located between 1472 cm^{-1} - 1457 cm^{-1} is compared to the sum of the integrated intensities of the gauche and trans (amorphous) bands between 1456 - 1466 cm^{-1}.[83] After deconvoluting the peaks using OMNIC software (Thermo Scientific), the percent crystallinity was then calculated using following relationship (Eq. 6)

$$X = 1 - \frac{\left(\frac{1-\frac{I_{cr}}{I_{am}}}{1.233}\right)}{1+\frac{I_{cr}}{I_{am}}} \times 100 \quad (6)$$

where X represents the percent crystallinity component, I_{cr} is the integrated area of the crystalline region, I_{am} is the sum of the integrated areas of the amorphous region and 1.233 is the calculated intensity ratio of I_{cr}/I_{am}.[84] The Omnic functions “Find Peaks” and “Fix Peaks” (Appendix) were used to determine the values for I_{am} and I_{cr}.

A similar peak resolving technique using OMNIC software was also used to assess PET’s crystallinity. The crystalline and amorphous bands for PET are located at 1717 cm^{-1} and 1727 cm^{-1}, respectively. This method was presented by Chen (2012)[85] and uses the area

of the two peaks to determine the ratio of the crystalline peak to the amorphous peak. Eqn. 7 was used to calculate the ratio of the two peak areas and is as follows,

$$Ratio\ of\ crystalline\ to\ amorphous = \frac{I_{cr}}{I_{am}} \quad (7)$$

where I_{cr} is the area of the crystalline peak at 1717 cm^{-1} and I_{am} is the area of the amorphous peak at 1727 cm^{-1}.[85] Unfortunately, there is not a normalization value in the literature like PE, so PET crystallinity is reported as a ratio instead of a percentage.

2.1.2.3 Surface Imaging

All polymer surfaces were analyzed using scanning electron microscopy (SEM). The plastic samples were coated with 10 nm of Au and scanned using a JEOL JSM-4690LV (Tokyo, Japan) scanning electron microscope at 10kV with a 600x zoom.

2.1.3 Batch Adsorption Experiments

Films of the desired polymer type were placed into a scintillation vial with on average 30 mg PE and 35 mg PET, then topped with a 1.5x1.5 cm piece of 20 gauge wire mesh purchased from Shanghai Yi Electromechanical Technology Co., Ltd (Zhejiang, China). The vial was then filled with 6 mL of a coumarin in ultrapure water solution of one of the five starting concentrations (1, 5, 10, 25, and 50 μM). The vials were then sealed with Parafilm M (Bemis Company, Neenah, Wisconsin). Vials were shaken in the dark at 30 ± 0.5 °C for 6 time intervals up to 36 days in a reciprocating shaker at 60 rpm. At the designated time points, the vials were opened, 100 μL of sample was taken, the caps were closed and sealed with Parafilm M, and the vial was placed back into the shaker immediately. All samples were performed in triplicate.

To assess molecule loss due to additional removal processes, i.e. sorption to glass wall and/or wire mesh, controls were shaken for the same time periods. No sorption was observed in the controls (Appendix) so results of sorption onto plastic samples did not need correction.

2.1.4 Chemical Analysis

The concentration of coumarin in the aqueous phase was determined by UPLC. LC analyses were done on a Waters Acquity Ultra Performance LC (Waters Corporation, Milford, Massachusetts). A Waters Acquity UPLC BEH C18 column with 1.7 μm particles (Waters Corporation, Milford, Massachusetts) was used for chromatographic separation. The UPLC method had a flow rate of 0.350 mL/min with 65% ultrapure water:35% acetonitrile.

2.1.5 Sorption Model

As discussed above, previous research states vapor permeability of small molecules amounts and diffusion rates being low and slow for polymers, specifically PE and PET.[52,86,87] The mechanism of sorption for coumarin to PE and PET is assumed to be adsorption. This is what lead to using the Freundlich and Langmuir isotherms to assess the polymers' sorption capacity. The batch experiments were determined to be at equilibrium after the concentration of the sorption solution did not change and no more loss was detected for several weeks. Then, the determined concentration adsorbed onto the plastic at equilibrium was calculated by using the highest concentration of coumarin at the beginning of the experiment and subtracting the equilibrium concentration. Each isotherm was able to be plotted by applying the mathematical manipulations from Eq. 2 and Eq. 4 for the Freundlich and Langmuir

models, respectively. Once the linear form of the Langmuir isotherm was plotted (Eqn. 4), the slope is inverted and multiplied by the y-intercept to get the distribution coefficient, K_d.

CHAPTER 2.2: RESULTS AND DISCUSSION

2.2.1 Adsorption Model Determination

It is important for the adsorption isotherm to be selected based on agreements between the theoretical prediction and the experimental results. Theoretically, it was predicted this experimental data would follow the Langmuir model as the assumptions with this model are expected to match polymer-sorbent system. This is not only because mono-layer coverage and adsorption to micro-voids is assumed, but a main doubt concerning the Freundlich isotherm is its assumption that infinite adsorption occurs with increasing sorbate concentration.[88] Therefore, the Langmuir isotherm was evaluated against one of the most commonly used isotherms, Freundlich, to validate the assumption. The chosen adsorption isotherm truly depends on the chemical and plastic pairing and should be determined by the one with the better fit and most accurate assumptions.[89-91] Therefore, after plotting (Figure 2.1, 2.2, and Appendix) the Langmuir and Freundlich isotherms were compared with linear regression for all polymer sample types in order to choose the appropriate adsorption model. The values for the standard errors for each experiment are listed in Table 2.1.

Table 2.1. Standard error values of linear regressions for Freundlich and Langmuir isotherms.

Irradiation Time (h)	**PE (L/g)**		**PET (L/g)**	
	Freundlich	Langmuir	Freundlich	Langmuir
0	0.076	0.168	0.166	0.170
24	0.520	0.006	0.048	0.155
48	0.394	0.157	0.404	0.203
72	0.263	0.123	0.238	0.097

The Langmuir standard error values were lower or within 5% of the Freundlich isotherm for all polymers except non-irradiated and 24 h UV PE. Although these polymers had lower standard error using the Freundlich isotherm, the Langmuir model was still used to determine the distribution constant because the error with the Langmuir model was still low and the assumptions of the Langmuir model are more appropriate for the polymer-sorbent system.

2.2.2 Distribution Coefficient Determination

The adsorption data for PE and PET was plotted to get a visual representation of the adsorption behavior. The results can be seen in Figure 2.1 and 2.2 for PE and PET, respectively.

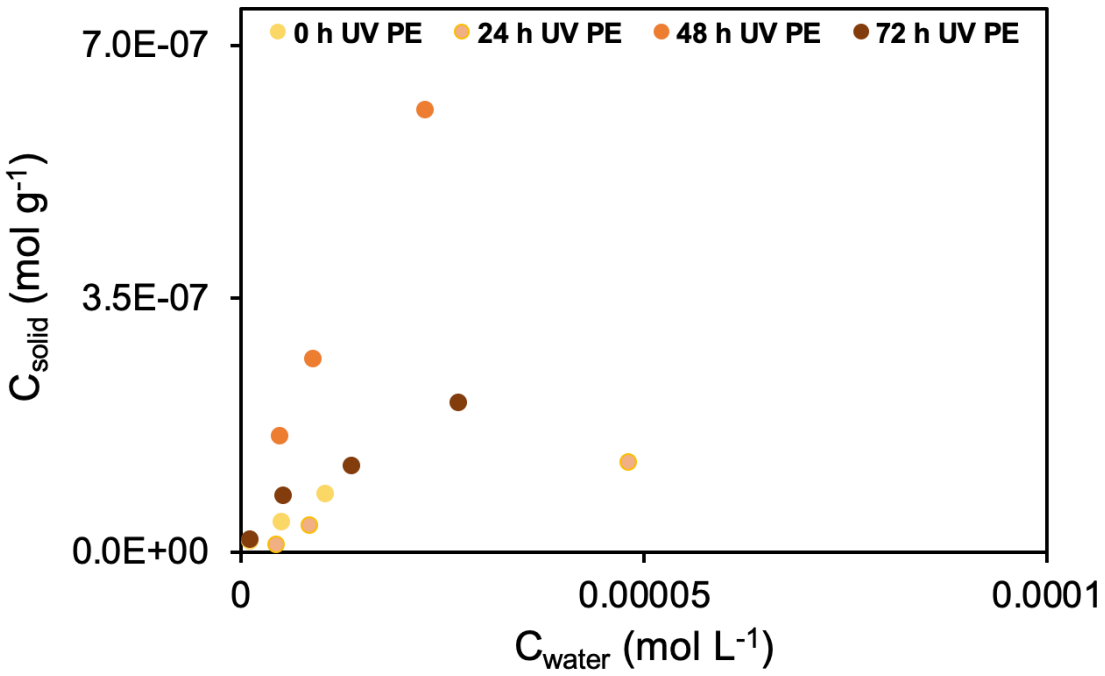

Figure 2.1: Adsorption data for 0, 24, 48, and 72 hours of irradiation of PE.

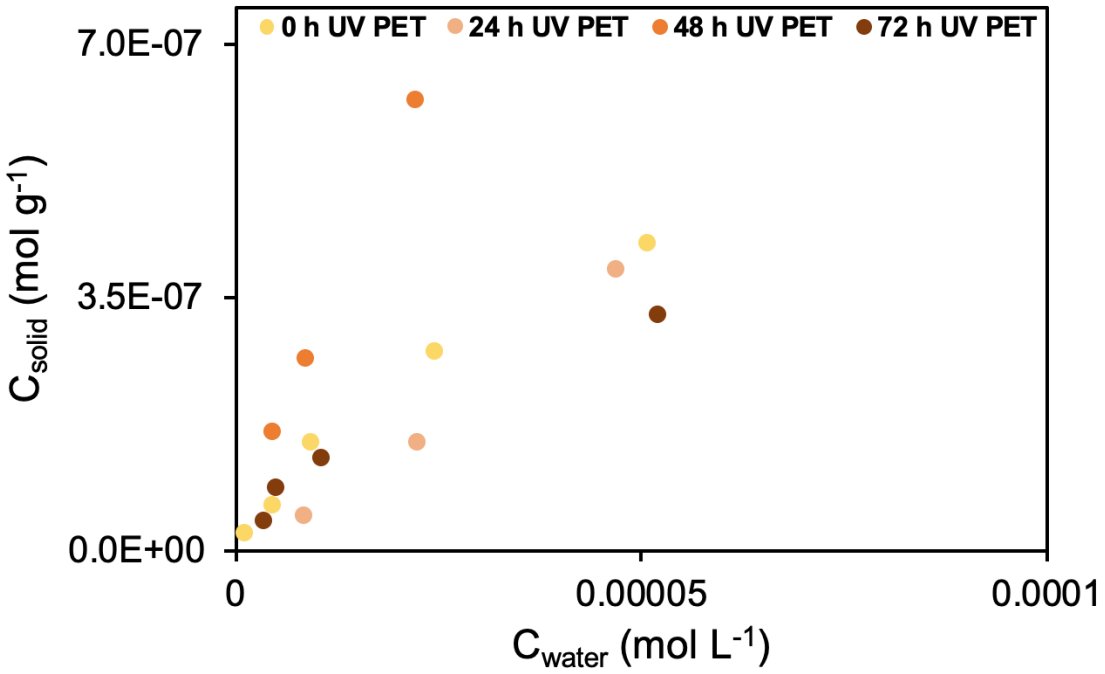

Figure 2.2: Adsorption data for 0, 24, 48, and 72 hours of irradiation of PET.

The shape of the data indicates that the Langmuir isotherm would be valid to assess the polymer distribution coefficients. This is because the data does not stay linear as the Freundlich isotherm would predict. Polymers samples' distribution coefficients, K_d, were therefore calculated using the linearized form of the Langmuir isotherm and the results can be seen in Table 2.2 and Figure 2.3. For both PE and PET, an initial decrease through 24 hours occurred. For PE, this decrease of K_d continued until the 48 h time point and then increase at 72 h to a value higher than non-irradiated PE. For PET, the K_d values increased from 24 to 48 h as well as from 48 to 72 h. Similar to PE, the 72 h PE, PET's 72 h sample K_d was higher than that of its non-irradiated form.

Table 2.2. Distribution coefficients for PE and PET samples.

Irradiation Time (h)	PE (L/kg)	PET (L/kg)
0	30.26	31.83
24	24.69	8.33
48	12.50	12.94
72	37.74	34.94

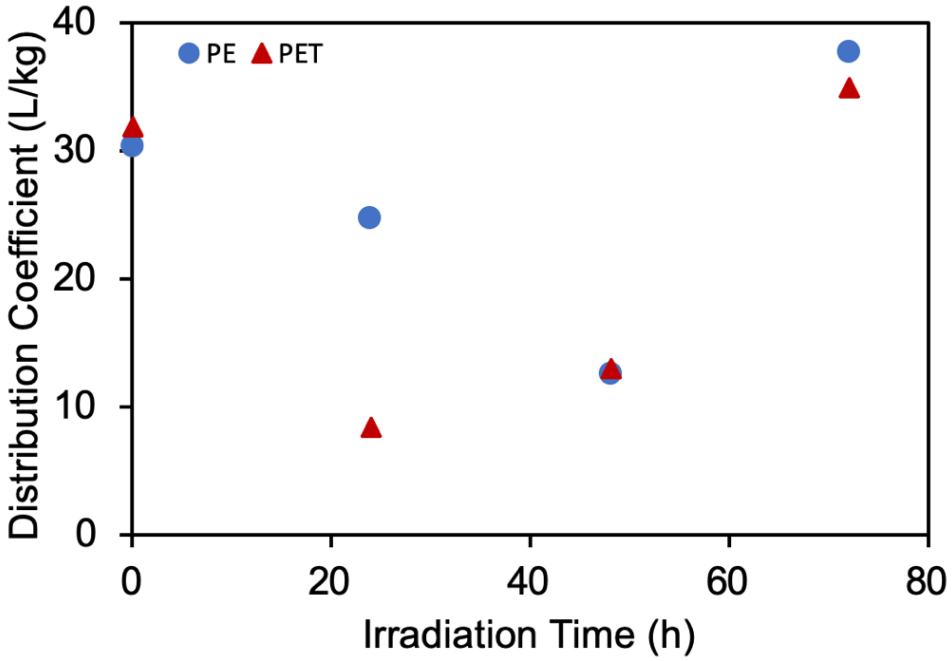

Figure 2.3: Distribution coefficients, K_d, for PE and PET upon irradiation.

Table 2.3 shows literature values of distribution coefficients for different sorbates to PE. Although adsorption data with PE and sorbates with $\log K_{ow}$ values less than two are sparse, trends observed in literature show that the distribution coefficients will decrease with decreasing $\log K_{ow}$ values. [74,92,93] Therefore, since coumarin has a $\log K_{ow} = 1.39$, its partitioning coefficient with PE would be predicted to be less than benzene that has a $\log K_{ow} = 2.13$. The K_d for coumarin with non-irradiated PE was 30.26 L/kg for this experiment therefore following the results and identified trend through previous research.

Table 2.3. Values of $\log K_{ow}$ for sorbates and $K_{d,PE}$ values from various sources.

Sorbate	**$\log K_{ow}$**	**$K_{d,PE}$ (L/kg)**	**Source**
Toluene	2.73	104.7	Saquing et al. 2010 [94]
Carbamazepine	2.45	191	Wu et al. 2015 [92]
Tribromomethane	2.40	75.86	EPA 2012 [93]
Benzene	2.13	44.67	EPA 2012 [93]

2.2.3 Polymer Characterization

In order to gain a better understanding of the distribution coefficient behavior, the coefficients were compared to the polymers' structural changes upon photodegradation. The main characteristics thought to affect adsorption analyzed in this research were hydrophobicity and crystallinity. The following sections discuss each of the characteristics and their relationship with the distribution coefficients in more depth.

2.2.3.1 Hydrophobicity

As mentioned previously, the formation of oxygen groups like carbonyls, hydroxyls, and carboxylic end groups on the polymer surface increases hydrophilic character.[63,64] This increase of hydrophilicity is hypothesized to negatively affect the adsorption of hydrophobic contaminants therefore making it important to understand the change in polymer hydrophobicity. The hydrophobicity of the polymer samples was generalized to the amount of polar moieties on their surface. For PE, its hydrophobicity was characterized using the carbonyl index. However, as discussed earlier CI is not a good measure of hydrophobicity for PET, so the change in content of another moiety, specifically the hydroxyl group, was quantified. CI is calculated using FTIR spectra, Figure 2.4. Figure 2.1.4a shows the entire IR spectra of PE. Figure 2.4b and c are two main regions that large changes to spectral bands are observed. For CI, the focus is in the region pictured in Figure 2.4b, the carbonyl region between 1600 and 1850 cm^{-1}.

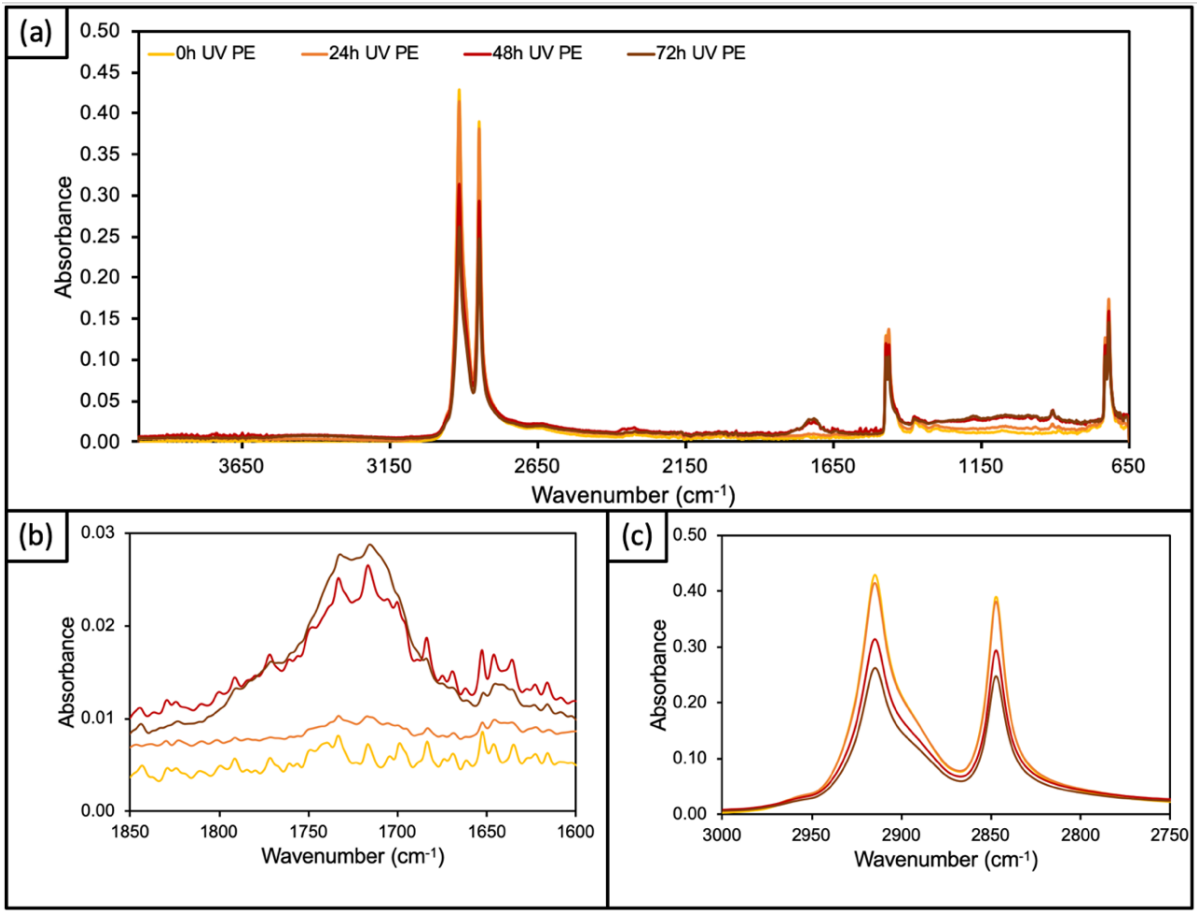

Figure 2.4: (a) Full ATR-FTIR Spectrum 650 to 4000 cm^{-1}, (b) carbonyl region of 0 h irradiated to 72 h irradiated PE, (c) -CH_2- asymmetric and symmetric stretching of 0 h irradiated to 72 h irradiated PE.

Looking at Figure 2.4b, the carbonyl region increases as the amount of UV irradiation increases. This can be explained by the oxidation that occurs from UV degradation that forms carbonyl groups on PE's chains. The result for determining the CI can be seen in Table 2.4 and Figure 2.5. As predicted, increased irradiation time causes an apparent increase in CI, up to at least 72 h which in turn decreases the PE hydrophobicity.

Table 2.4. CI of PE from 0 to 72 h of irradiation obtained using ATR-FTIR.

Irradiation Time (h)	CI
0	0
24	0.412
48	2.414
72	4.653

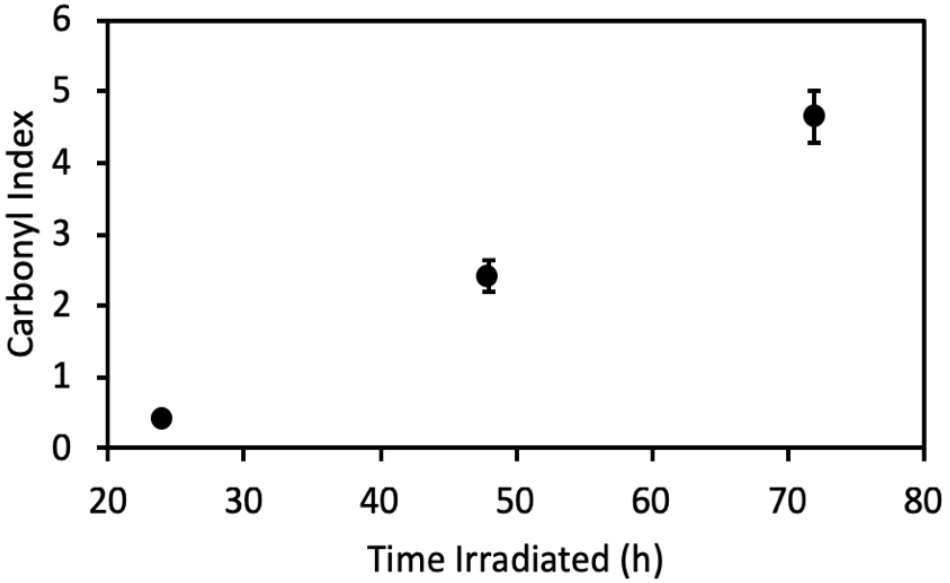

Figure 2.5: Carbonyl index for PE as a function of irradiation time. Markers represent average percent crystallinity of 3 scans with error bars representing the standard deviation.

The ATR-FTIR spectra for PET samples can be seen in Figure 2.6. Since PET already contains ester groups within the polymer backbone structure, its predicted initial hydrophobicity is less than non-irradiated PE. With irradiation, the IR spectra of PET shows an increase in the hydroxyl area (Figure 2.6b). Bands at 1235 cm^{-1} and 1090 cm^{-1} correspond to C(=O)-O and C-O stretching, respectively.[95] In Figure 2.6c, there is an increase of ether groups and C-O stretching bands, indicating an increase in their content. The increase of these hydrophilic moieties indicates that PET is getting less hydrophobic with the increase of irradiation time.

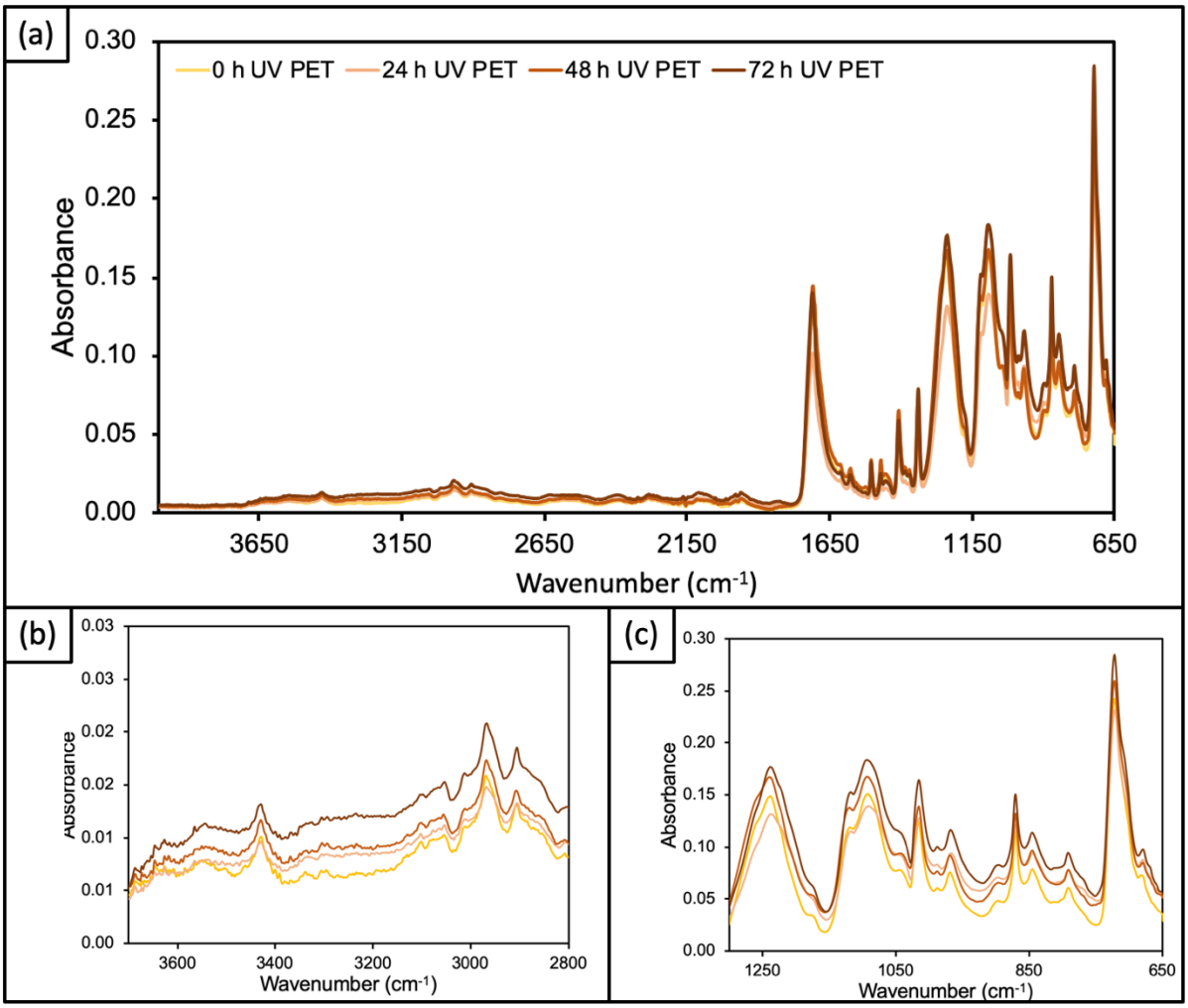

Figure 2.6: (a) Full ATR-FTIR spectra, (b) Hydroxyl region, and (c) Fingerprint region of 0 h irradiated to 72 h irradiated PET.

Because PET contains carbonyl moieties as part of the ester linkages, the CI cannot accurately quantify PET oxidation. Therefore, fluorescence spectroscopy was used to analyze oxidation, quantifying the formation of the fluorogenic, mono-hydroxylated species that forms with photodegradation. Figure 2.7 shows the fluorescence spectra obtained of irradiated PET samples, with the fluorescent product forming at a maximum emission wavelength of 460 nm. The increase in emission intensity means there is an increased presence of hydroxy groups, therefore increased polymer hydrophilicity.

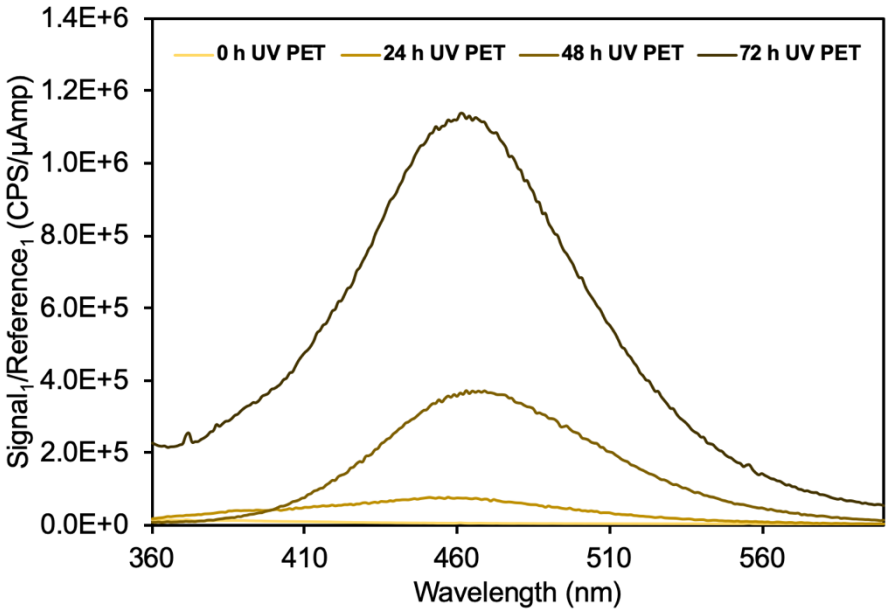

Figure 2.7: Fluorescence emission spectra of non- and irradiated PET (excitation, 360 nm).

The peak area of the emission band was obtained to get a value for approximating the amount of mono-hydroxylated terephthalate species for each irradiation time, therefore relative hydrophobic character. The integration results can be seen in Table 2.5 and Figure 2.8. It can be noted that the increase of mono-hydroxylated compound emission area for these irradiation timepoints is not linear with time, but rather looks like an exponential relationship. This means the rate of mono-hydroxylated compound formation gets faster as irradiation time increases.

Table 2.5. Emission area of monohydroxylated terephthalate compound in reference to PET irradiation time.

Irradiation Time (h)	Area of Monohydroxylated Terephthalate Compound Emission (CPS/µAmp)
0	9.80×10^4
24	8.34×10^6
48	3.07×10^7
72	9.27×10^7

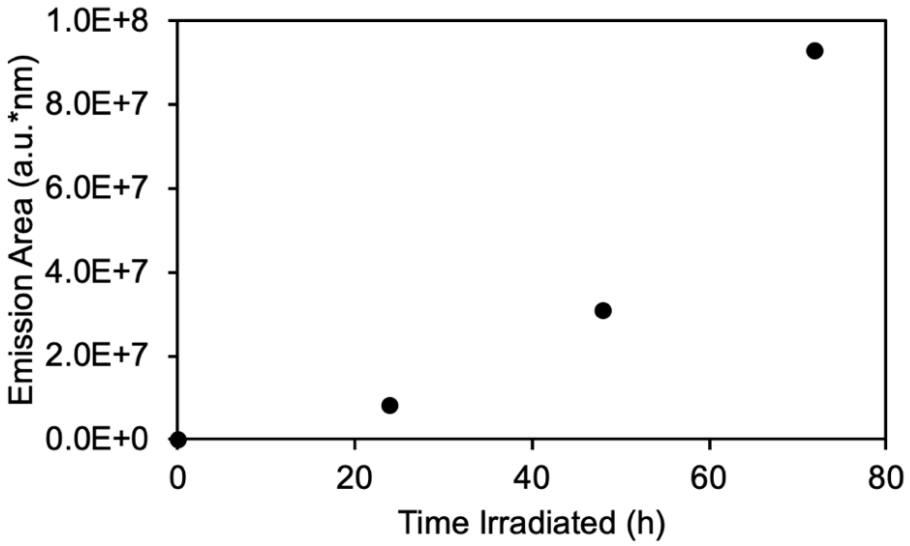

Figure 2.8: Peak area of monohydroxylated PET compound.

In order to correlate the trends of coumarin adsorption to irradiated polymers, the distribution coefficients for both PE and PET were compared to their indicators of hydrophobicity, Figure 2.9.

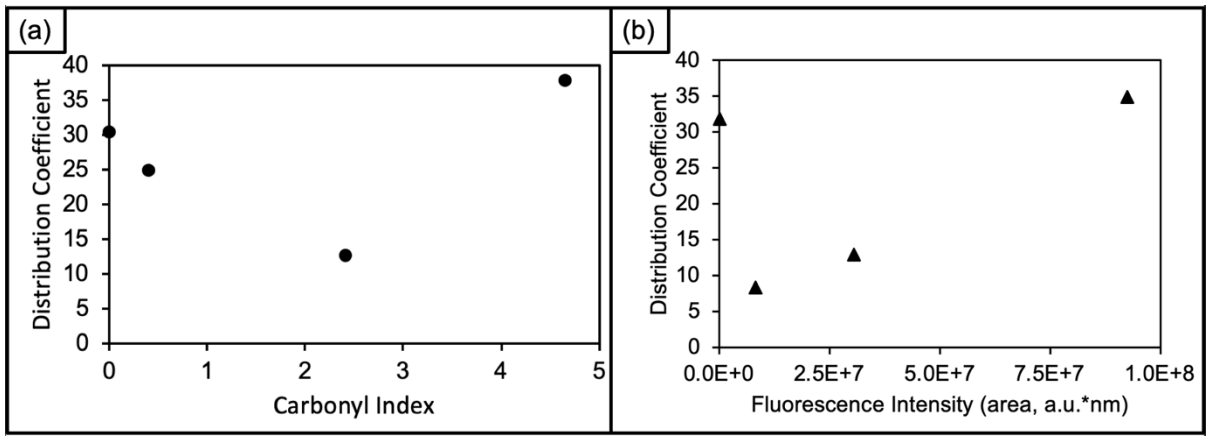

Figure 2.9: (a) Comparison of PE's Carbonyl index at 0, 24, 48, and 72 hours of irradiation (left to right) to its respective distribution coefficient. (b) Comparison of PET's monohydroxylated compound fluorescence emission area at 0, 24, 48, and 72 hours of irradiation (left to right) to its respective distribution coefficient.

The lack of correlation suggests adsorption related to hydrophobicity is a complex relationship and likely, there is more than one dominating phototransformation causing the changes to K_d. Referring back to Figure 2.3, the initial decrease in K_d observed for either polymer upon irradiation can be supported from the decrease in hydrophobic character. The increase of polymer hydrophilicity is predicted to lower sorption capabilities with respect to a hydrophobic molecule, specifically coumarin ($\log K_{ow} = 1.39$). For PET, the initial K_d decrease is at a much larger magnitude than PE. This may indicate either the rate of these phototransformations are larger for PET or, that the change of hydrophobicity of PET more strongly affects the change in K_d.

For the non-irradiated time points, PET had a higher K_d for coumarin than PE. This does not match the initial hypothesis that PE, having a lower hydrophobicity than PET, would adsorb coumarin better. This leads to the hypothesis that hydrophobicity may not be as straightforward of a characteristic as posed. Not only can hydrophobicity change the interaction between model compound and polymer, but it also may change the ability for water to reach and penetrate the polymer. Previous studies have shown that with incorporation of oxygen comes enhances solubility of water,[86] as water wants to wet hydrophilic domains.[96] The increase of oxygen groups from photodegradation could therefore lead to higher water solubilities and surface wetting, increasing the amount of micropollutant making it to the surface. This may be why PET had a higher initial sorption than PE as its initial structure contains oxygen groups and PE's does not. This idea of wetting could also help explain why the earlier irradiation times with minimal incorporation of oxygen groups could lead to heterogenous wetting, decreasing the concentration of model micropollutant on the surface. Potentially, with enough oxygen groups in the later irradiation times, the wetting becomes more homogeneous and leads to a higher adsorption capacity.

The combination of increased wetting combined with increased surface area could also be an explanation why the distribution coefficients at the 72 h time point for PE and PET was higher than the initial, non-irradiated values.

2.2.3.2 Crystallinity

Previous studies have shown the diffusion ability of a chemical through a polymeric material decreases with increasing crystallinity.[81] Therefore, it is important to measure its changes when PE and PET are photodegraded. Bulk crystallinity was also measured with DSC and is demonstrated in the Appendix. However, because adsorption is a surface phenomenon and literature states surface behavior differs from bulk behavior of many materials,[97,98] As FTIR provides a more accurate depiction of surface crystallinity, crystallinity for the polymers was determined using ATR-FTIR. Polyethylene's percent crystallization increases with increasing irradiation time as can be seen in Table 2.6 Figure 2.10. The observed increase in crystallinity is likely due to the scission that occurs during photodegradation that leads to chemi-crystallization. It would then be predicted that the distribution coefficient would decrease with increasing crystallinity.

Table 2.6. Percent crystallinity of PE upon photodegradation obtained by ATR-FTIR.

Irradiation Time (h)	PE (%)
0	62.24
24	65.09
48	69.55
72	73.46

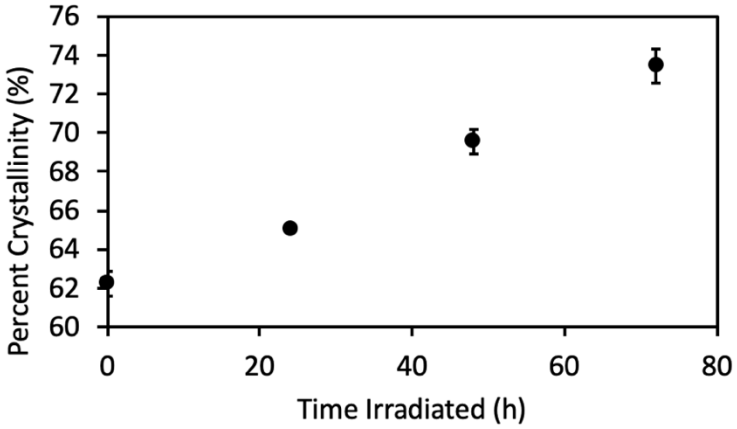

Figure 2.10: Percent crystallinity of PE as a function of irradiation time.

The analysis of PET also showed an increase of crystallinity upon irradiation. The results for the I_{cr}/I_{am} ratio obtained with FTIR can be seen in Table 2.7 and Figure 2.11. The observed increase of crystallinity is likely due to scission reactions PET undergoes upon irradiation and the molecular weight distribution for the longer irradiated polymers would decrease with respect to this photochemical transformation.

Table 2.7. Crystallinity ratio of PET upon photodegradation obtained by ATR-FTIR.

Irradiation Time (h)	PET
0	0.325
24	0.496
48	0.581
72	1.146

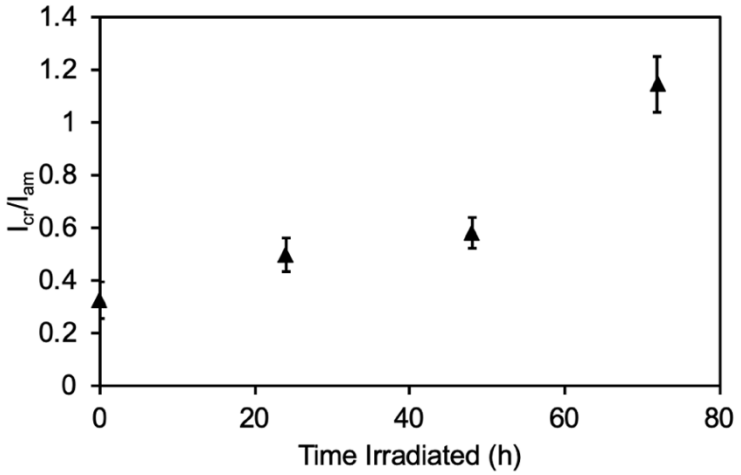

Figure 2.11: Crystallinity of PET calculated from amorphous and crystalline peak areas

Referring back to Figure 2.4.a, an increase in absorption was observed between about 700 and 1400 cm^{-1}, where a broad band appears as irradiation amount increases. This change within the IR spectra has been observed previously[99] but there has been no identified cause for this change. However, this portion of the IR spectra, often referred to as the fingerprint region, is the result of molecular vibrations caused by multiple bonds. It is hypothesized this increased band could be the result of crosslinking. This is supported within the paraffin literature where branched paraffin waxes have increased the bands in the 900-1100 cm^{-1} region.[100] Although crosslinking may be occurring, the increase in crystallinity suggests scission is the dominating pathway.

The distribution coefficients for both PE and PET were compared to the obtained values of crystallinity, Figure 2.12.

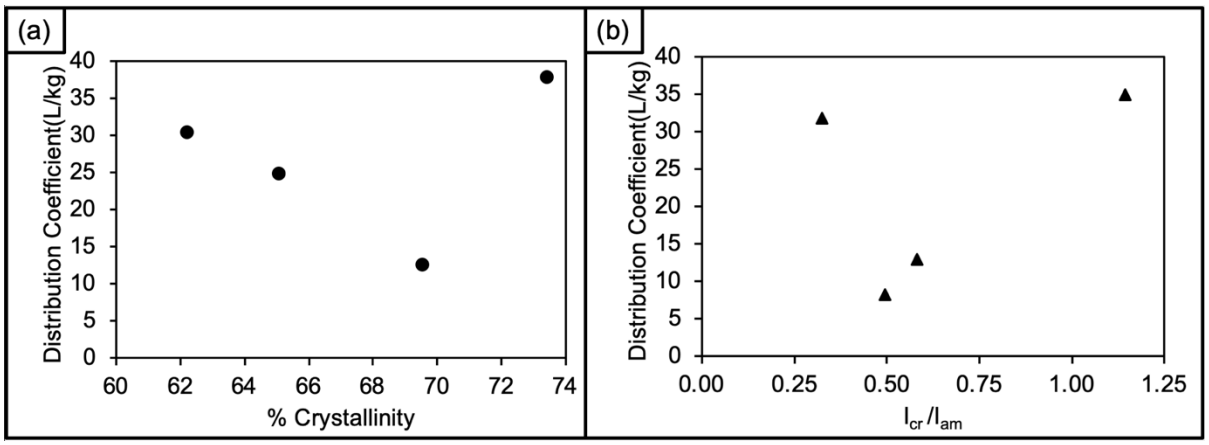

Figure 2.12: (a) Comparison of PE's percent crystallinity at 0, 24, 48, and 72 hours of irradiation (left to right) to its distribution coefficient. (b) Comparison of PET's ratio of crystalline band area to amorphous band area at 0, 24, 48, and 72 hours of irradiation (left to right) to its distribution coefficient.

Again, there is a lack of correlation to the distribution coefficient supporting the previously stated hypothesis that there is more than one dominating phototransformation affecting K_d. The initial decrease in K_d for PE and PET upon irradiation is supported by the crystallinity data as the crystallinity values increases for both polymers, recalling that the

increase in polymer crystallization is predicted to lower sorption capabilities. PET's increase of K_d beyond 24 h of irradiation cannot be linked to its decrease in hydrophobicity or crystallinity so another change of the polymers must be affecting the adsorption of coumarin. The new hypothesis is that surface area is increasing and overpowering the other photochemical changes.

2.2.3.3 Surface Analysis

Initially, pictures of the PE and PET samples were taken of samples to show any progression of yellowing. The results can be seen in Figure 2.13. No signs of yellowing were present in the PE samples (Figure 2.13a), but yellowing did occur as early as 24 hours of UV irradiation for PET (Figure 2.13b). The yellowing is believed to be a result from the formation of crosslinked products, which increases aromaticity and forms chromophoric biphenyls or benzaphenone molecules.[77] The yellowing however did not seem to dramatically increase with the time points past 24 hours. Beyond yellowing, it was observed that polyethylene became very brittle and fell apart easily by the 72-hour time point. PET, on the other hand, did not display brittleness even at 72 hours of irradiation.

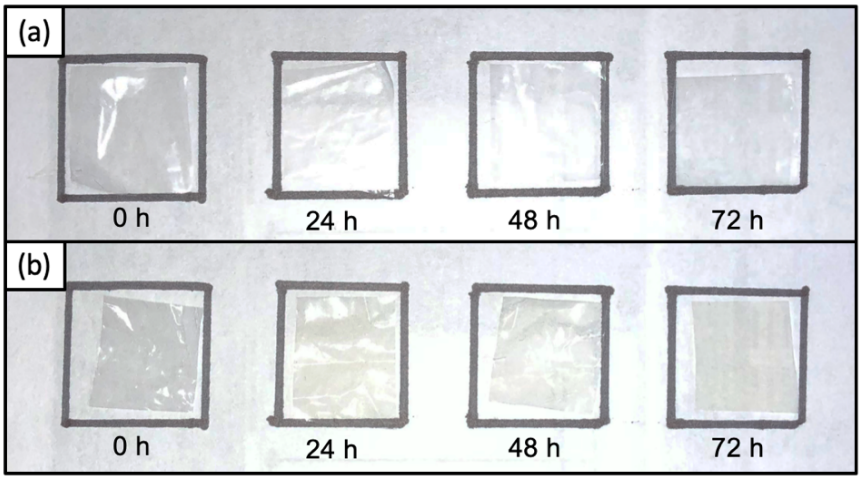

Figure 2.13: Photographs of (a) PE and (b) PET polymers after various amounts of 254 nm UV irradiation.

Further analysis of the polymer surfaces was done using SEM imaging. The results for all eight polymer types can be seen in Figure 2.14. Although the surfaces of non-irradiated PE and PET are different, both polymers begin to show increased surface roughness (e.g., scratches/cracks) as irradiation time increases. These signs of aging would increase the polymer surface area.

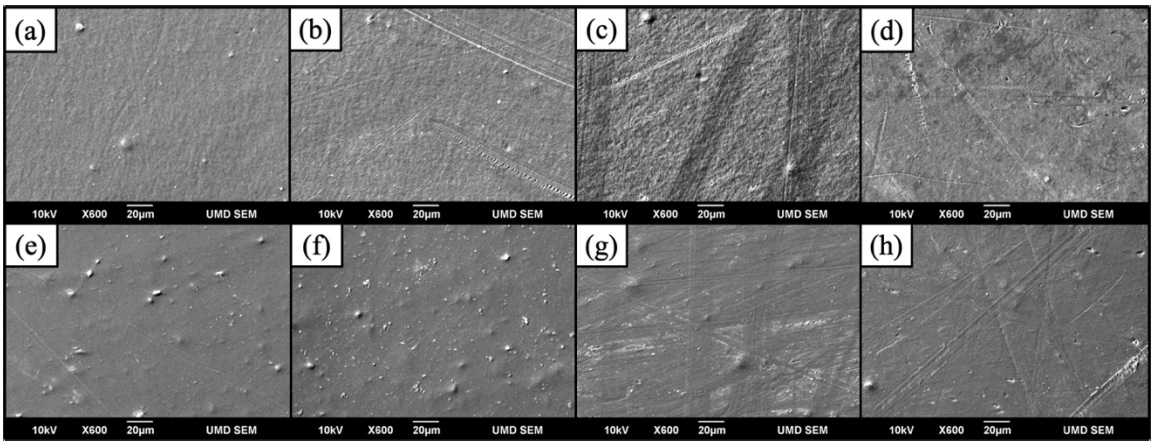

Figure 2.14: SEM images of polymers after 10 nm coating of Au where (a) Non-irradiated PE, (b) 24 h irradiated PE, (c) 48 h irradiated PE, (d) 72 h irradiated PE, (e) non-irradiated PET, (f) 24 h irradiated PET, (g) 48 h irradiated PET, (h) 72 h irradiated PET.

The assumption of pore formation can be supported using the results from Figure 2.4c, PE -CH_2- stretching. The values decrease as irradiation time increases. Unfortunately, literature does not dive into the likely cause of this decrease, but the hypothesis is that this decrease may be the result from an increase of pore formation or increased surface roughness upon photodegradation supported by the decrease in area of the CI normalization band (1380 cm^{-1}) with the increase of irradiation time (Table 2.8).

Table 2.8: Average areas of normalization band (1380 cm^{-1}) from IR spectra of irradiated PE.

Irradiation Time (h)	Normalization Band Area[a] (a.u.*cm^{-1})
0	0.382 ± 0.012
24	0.358 ± 0.019
48	0.276 ± 0.048
72	0.228 ± 0.015

[a]Area represents average ± standard deviation of 6 spectra replicates

More pores may result in an absorbance intensity decrease as less of the polymer is in contact with the FTIR beam.

Upon further investigation, many applications were found where adsorbent materials were affected by surface area. For example, activated carbon is frequently used to adsorb impurities from a different phase and its efficiency of adsorption is known to be dependent on surface area.[101,102] A study done by Fotopoulou and Karapanagioti found an increase of surface areas for beach eroded PP and PE increased the adsorption capacity of the plastic.[103] This makes it increasingly clear that the surface area of these irradiated polymers needs to be further studied to assess the impact of surface area in this study.

CHAPTER 2.3: CONCLUSION AND FUTURE DIRECTIONS

Plastic pollution is an increasing environmental concern, especially to marine organisms. The addition of persistent environmental contaminants along with the ability for polymers to sorb these contaminants creates another important concern. Although an increasing number of studies have pursued quantifying sorption with common marine plastics, the work presented herein offers a new understanding of the dynamics that photodegradation plays on the sorption to plastics.

Specifically, this work assessed the effects of changing PE and PET hydrophobicity and crystallinity via UV degradation and in turn, how these phototransformations effected their sorption abilities with coumarin. Both hydrophobicity and crystallinity were found to continually increase for PE and PET, yet the distribution coefficient did not continually decrease as predicted. The results of these experiments suggest hydrophobicity and crystallinity do not solely affect adsorption and that surface area and wetting have impact it

as well. The observed increase of the distribution coefficient was therefore determined to be connected to the increase of surface area.

In future work, it is important to complete similar experiments with a variety of model pollutants with differing K_{ow} values. This will help assess the impact of compound hydrophobicity as well as polymer hydrophobicity on adsorption. Using other model micropollutants would also test if the initial decrease then increase of K_d values with increasing irradiation time occurs with other contaminants.

Because of the lack of dependence found from hydrophobicity and crystallinity, it will be important to quantify the surface area of the polymers to assess the magnitude of its role during adsorption processes. It is also important to consider that the methods used for characterizing hydrophobicity and crystallinity may not be the best representation for these kinds of phototransformations. Assessment of the relationship for CI and fluorescence measurements between PE and PET's contact angle measurement would be a way look at how these types of measurements relate to hydrophobicity. In turn, it would be beneficial if contributions to adsorption patterns from crystallinity and hydrophobicity could be deconvoluted, but there is not an obvious path to do so at this time.

Another direction to take this project would be to examine the solution of the irradiated polymers, specifically PET, after they have been in the vials for several days. In the irradiated polymer chromatograms, there are other compounds present that are not coumarin after 7 days in solution (Appendix). Studying these leachates with LC-MS would give more information about how the polymers degrade or fragment and therefore give insight to adsorption changes upon photodegradation.

Another impactful direction would be to add salts or dissolved organic matter to the adsorption solutions to be more relevant to marine envirionments. Overall the preliminary

data indicates there is a clear need to keep evaluating the effects of polymer photo-degradation on plastic sorption abilities in order to better understand the fate of plastics and pollutants in the marine environment.

References

1. Geyer, R.; Jambeck, J.; Law, K. Production, use, and fate of all plastics ever made. *Science Advances.* **2017.** 3, n.p.
2. Sarker, M.,;Rashid, M.; Rahman, M.; Molla, M. Polypropylene waste plastic into light fractional gasoline grade fuel for vehicle by using two step thermal process. *International Journal of Forest, Soil and Erosion (IJFSE).* **2012.** 2(4), 186–191.
3. Jambeck, J. et al. Plastic waste inputs from land into the ocean. *Science.* **2015.** 347, 768–771.
4. Law, K. et al. Plastic accumulation in the North Atlantic subtropical gyre. *Science.* **2010.** 329, 1185-1188.
5. Thompson, R. et al. Lost at sea: Where is all the plastic? *Science.* **2004.** 304, 838.
6. Lang, G. Plastics, the marine menace: causes and cures. *Journal of Land Use & Environmental Law.* **1990.** 5(2), 729-752.
7. Rillig, M. Microplastic in terrestrial ecosystems and the soil? *Environ. Sci. Technol.* **2012.** 46(12), 6453-6454.
8. Graham, E.; Thompson, J. Deposit- and suspension-feeding sea cucumbers (Echinodermata) ingest plastic fragments. *Journal of Experimental Marine Biology and Ecology.* **2009.** 368 (1), 22-29.
9. Ryan, P.G. et al. Monitoring the abundance of plastic debris in the marine environment. *Philos. T. Roy. Soc. B.* **2009.** 364, 1999-2012.
10. Barnes, D.; Galgani F.; Thompson, R.; Barlaz, M. Accumulation and fragmentation of plastic debris in global environments. *Philos Trans R Soc Lond B Biol Sci.* **2009.** 364, 1985–1998.
11. Erikson, M. et al. Plastic pollution in the world's oceans: more than 5 trillion plastic pieces weighing over 250,000 tons afloat at sea. *PLoS One.* **2014.** 9(12): 111913.
12. Rochman, C. et al. Scientific evidence supports a ban on microbeads. *Environ. Sci. Technol.* **2015.** 49(18), 10759-10761.
13. Dubaish, F.; Liebezeit, G. Suspended Microplastics and Black Carbon Particles in the Jade 556 System, Southern North Sea. *Water Air Soil Pollut.* **2013.** 224, 1-8.
14. Wagner, M. et al. Microplastics in freshwater ecosystems: What we know and what we need to know. *Environ. Sci. Eur.* **2014.** 26, 12.
15. Bletter, M. et al. Plastic pollution in freshwater ecosystems: macro-, meso-, and microplastic debris in a floodplain lake. *Envrion. Monitoring and Assessment.* **2017.** 189(11): 581.
16. Dris, R. et al. Beyond the Ocean: Contamination of freshwater ecosystems with (micro-) plastic particles. *Environ. Chem.* **2015.** 12, 539-550.
17. Teuten, E. et al. Potential for plastics to transport hydrophobic contaminants. *Environ. Sci. Technol.* **2007.** 41(22), 7759-7764.
18. Browne, M. et al. Ingested microscopic plastic translocates to the circulatory system of the mussel, Mytilius edulis (L.). *Environ. Sci. Technol.* **2008.** 42(13), 5026-5031.
19. Imhof, H. et al. Contamination of beach sediments of a subalpine lake with microplastic particles. *Current Biology.* **2013.** 23(19), 867-868.

20. Wright, S.; Thompson, R.; Galloway, T. The physical impacts of microplastics on marine organisms: a review. *Environmental Pollution.* **2013.** 127, 483-492.

21. Laist, D. *Impacts of marine debris: entanglement of marine life in marine debris including a comprehensive list of species with entanglement and ingestion records.* In: Coe, J.M., Rogers, D.B. (Eds.), Marine Debris sources, Impacts and Solutions. Springer-Verlag New York Inc.: New York, 1997.

22. Cole, M. et al. Microplastic ingestion by zooplankton. *Environ. Sci. Tech.* **2013.** 47, 6646-6655.

23. Derraik, J. The pollution of Marine Environment by Plastic Debris: A Review. *Marine Pollution Bulletin*. **2002.** 44, 842-852.

24. Moser, M; Lee, D. A fourteen-year survey of plastic ingestion by western North Atlantic seabirds. *Colonial Waterbirds.* **1992.** 12, 83-94.

25. Slip et al. Ingestion of anthropogenic articles by seabirds at Macquarie Island. *Marine Ornithology.* **1990.** 18, 74-77.

26. Webb, H. et al. Plastic degradation and its environmental implications with special reference to poly(ethylene terephthalate). *Polymers.* **2012.** 5, 1-18.

27. Wolfe, D. Persistent plastics and debris in the ocean: an international problem of ocean disposal. *Marine Pollution Bulletin.* **1987.** 18, 303-305.

28. Rochman, C. et al. Long-term field measurements of sorption of organic contaminants to five types of plastic pellets: Implications for plastic marine debris. *Environ. Sci. Technol.* **2013.** 47, 1646-1654.

29. Lee, H. et al. Sorption capacity of plastic debris for hydrophobic organic chemicals. *Sci Total Environ.* **2014.** 470, 1545-1552.

30. Bakir, A. et al. Competitive sorption of persistent organic pollutants onto microplastics in the marine environment. *Marine Pollution Bulletin.* **2012.** 64, 278-2789.

31. Rios, L. M.; Moore, C. J.; Jones, P. R. Persistent organic pollutants carried by Synthetic polymers in the ocean environment. *Mar. Pollut. Bull.* **2007,** 54 (8), 1230−1237.

32. Sheavly, S. B.; Register, K. M. Marine Debris and Plastics: Environmental Concerns, Sources, Impacts and Solutions. *J. Polym. Environ.* **2007.** 15 (4), 301−305.

33. Hirai, H.; Takada, H.; Ogata, Y.; Yamashita, R.; Mizukawa, K.; Saha, M.; Kwan, C.; Moore, C.; Gray, H.; Laursen, D.; Zettler, E. R.; et al. Organic micropollutants in marine plastics debris from the open ocean and remote and urban beaches. *Mar. Pollut. Bull.* **2011.** 62 (8), 1683−1692.

34. Takada, H. et al. Pellet Watch: Global monitoring of persistent organic pollutants (POPs) using beached plastic resin pellets. *The Plastic Debris Rivers to Sea Conference: Focusing on Land-Based Sources of Marine Debris, Redondo Beach, CA,* ***September 7-9, 2005.***

35. Gouin, T. et al. A thermodynamic approach for assessing environmental exposure of chemicals absorbed to microplastic. *Environ. Sci. Technol.* **2011.** 45(4), 1466-1472.

36. Zitko, V. Expanded polystyrene as a source of contaminants. *Marine Pollution Bulletin.* **1993.** 26, 583-585.

37. Andrady, A. L. Microplastics in the marine environment. *Mar. Pollut. Bull.* **2011.** 62 (8), 1596−1605.

38. Teuten, E. et al. Transport and release of chemicals from plastics to the environment and to wildlife. *Philos. Trans. R. Soc. London, Ser. B*. **2009.** 364 (1526), 2027−2045.

39. Mato, Y.; Isobe, T.; Takada, H.; Kanehiro, H.; Ohtake, C.; Kaminuma, T. Plastic Resin Pellets as a Transport Medium for Toxic Chemicals in the Marine Environment. *Environ. Sci. Technol.* **2001.** 35 (2), 318−324.

40. Betts, K. Why small plastic particles may pose a big problem in the oceans. *Environ. Sci. Technol.* **2008.** 42 (24), 8995−8995.

41. Frias, J. P. G. L.; Sobral, P.; Ferreira, A. M. Organic pollutants in microplastics from two beaches of the Portuguese coast. *Mar. Pollut. Bull.* **2010.** 60 (11), 1988−1992.

42. Chen, Q. et al. Pollutants in plastics within the north pacific subtropical gyre. *Environ. Sci. Technol.* **2018.** 52(2), 446-456.

43. Besseling, E. et al. Effects of microplastic on fitness and PCB bioaccumulation by the lugworm Arenicola marina (L.). *Environ. Sci. Technol.* **2013.** 42(13), 5026-5031.

44. Rochman, C. et al. Ingested plastic transfers hazardous chemicals to fish and induces hepatic stress. *Sci. Rep.* **2013.** 3, 3263.

45. Rochman, C. et al. Early warning signs of endocrine disruption in adult fish from the ingestion of polyethylene with and without sorbed chemical pollutants from the marine environment. *Sci. Total Environ.* **2014.** 493: 656661.

46. Schecter, A. et al. Perfluorinated compounds, polychlorinated biphenyls, and organochlorine pesticide contamination in composite food samples from Dallas, Texas, USA. *Environ. Health Perspect.***2010.** 118, 796-802

47. Trudel, D. et al. Total consumer exposure to polybrominated diphenyl ethers in North America and Europe. *Envrion. Sci. Technol.* **2011.** 45, 2391-2397.

48. Chung, S. Y. et al. Effects of grilling and roasting on the levels of polycyclic aromatic hydrocarbons in beef and pork. *Food Chem.* **2011.** 129, 1420-1426.

49. Zhou, Q.; Gao, Y.; Xie, G. Determination of bisphenol A, 4-n-nonylphenol, and 4-tert-octylphenol by temperature-controlled ionic liquid dispersive liquid-phase microextraction combined with high performance liquid chromatography-fluorescence detector. *Talanta.* **2011.** 85, 1598-1602.

50. Stern, S. Polymers for gas separations: the next decade. *J. Membr. Sci.* **1996.** 94, 1-65.

51. Bungay, P.; Lonsdale, H.; Pinho, M. Synthetic membranes: science, engineering, and applications. *NATO ASI Series.* **1983.** 181, np.

52. Kamal, M. Permeability of oxygen and water vapor through polyethylene/polyamide films. *Polymer Engineering and Science.* **1984.** 24917), 1340-1350.

53. Haymaker, J.; Thompson, J. *Organic chemicals in the Environment*; M. Dekker: New York, 1972.

54. Cornelissen, G. et al. The temperature dependence of slow adsorption and desorption kinetics of organic compounds in sediments. *Environ. Technol. Sci.***1997.** 31, 454-460.

55. Werth, C.; Reinhard, M. Effects of temperature on trichloroethylene desorption on silica gel and natural sediments. *Environ. Technol. Sci.* **1997.** 31, 697-703.

56. Van Bemmelen, J. Die adsorptionverbindugen und das adsorptionvermogen der ackererde. *Die Landwirtschat-lichenVersuchs-Stationen.* **1888.** 35, 69-136.

57. Freundlich, H. Kapillarchemie. Akademische verlagsge-sellschaft, Leipzig, Germany. **1909.**

58. Schwarzenbach, R.; Gschwend, P.; Imboden, G. *Environmental Organic Chemistry*, 3rd, Ed.; Wiley: New Jersey, USA, 2017.

59. Albalak, R. *Polymer Devolatiliation,* 1st, Ed.; Marcel Dekker: New York, USA, 1996.

60. Weber Jr., W. et al. Sorption phenomena in subsurface systems: concepts, models, and effects on contaminant fate and transport. *Wat. Res.* **1991.** 25(5), 499-528.

61. Hawkins, W.; Matreyek, W. The morphology of semicrystalline polymers. Part I. The effect of temperature on the oxidation of polyolefins. *J. Polym. Sci.* **1959.** 41, 1-11.

62. Gardette, M. et al. Photo- and thermal oxidation of polyethylene: comparison of mechanisms and influence of unsaturation content. *Polym. Degrad. Stabil.* **2013.** 98, 2383-2390.

63. Inagaki, N. *Plasma surface modification and plasma polymerization,* 1st ed.; CRC Press: Boca Raton, 1996.

64. Scheirs, J. *Compositional and failure analysis of polymers: a practical approach,* 1st ed.; John Wiley & Sons, Ltd.: West Sussex, 2000.

65. Fechine, G. J. M. et al. Surface characterization of photodegraded poly(ethylene terephthalate). The effect of ultraviolet absorbers. *Polymer.***2004.** 45, 2303-2308.

66. Geuskens, G.; Kabamba, M. Photo-oxidation of polymers—Part V: A new chain scission mechanism in polyolefins. *Polym. Degrad. Stabi.* **1982.** 4, 69–76.

67. Lewandowski, S.; Rejsek-Riba, V.; Bernes, A.; Perraud, S.; Lacabanne, C. Influence of environment during a photodegradation of multilayer films (PET). *J. App. Polym. Sci.* **2016.** 133, np.

68. Yousif, E.; Haddad, R.; Photodegradation and photostabilization of polymers, especially polystyrene: review. *SpringerPlus.* **2013.** 2, 389.

69. Day, M.; Wiles, D. Photochemical degradation of poly(ethylene terephthalate). II. Effect of Wavelength and environment on the decomposition process. *J. App. Polym. Sci.* **1972.** 16, 191-202.

70. Luongo, J. Effect of oxidation on polyethylene morphology. *J. Polym. Sci.* **1963.** 1, 141-143.

71. Carlsson, D.; Wiles, D. Photooxidation of polypropylene films. IV. Surface changes by attenuated total reflection spectroscopy. *Macromolecules.* **1970.** 4(2), 174-179.

72. Rabello, M.; White, J. Crystallization and melting behaviour of photodegraded polypropylene – I. Chemi-crystallization. *Polymer.* **1997.** 38(26), 6379-6387.

73. Fries, E.; Zarfl, C. Sorption of polycyclic aromatic hydrocarbons (PAHs) to low and high density polyethylene (PE). *Environ. Sci. Pollut. Res.* **2012.** 19, p1296-1304.

74. Guo, X. et al. Sorption of four hydrophobic organic compounds by three chemically distinct polymers: role of chemical and physical composition. *Environ. Sci. Technol.* **2012.** 46(13), 7252-7259.

75. Singh, A. Irradiation of polyethylene: some aspects of crosslinking and oxidative degradation. *Radiation Phys. And Chem.* **1999.** 56, 375-380.

76. Day, M.; Wiles, D. Photochemical degradation of poly(ethylene terephthalate). I. Irradiation experiments with the xenon and carbon arc. *J. App. Polym. Sci.* **1972.** 16, 175-189.

77. Bengough, W.; Sharpe, H. The thermal degradation of polyvinyl chloride in solution. II. The kinetics of the crosslinking reaction. *Macro. Chem. Phys.* **1963.** 66, 45-55.

78. Badr, Y. et al. Characterization of gamma irradiated polyethylene films by DSC and X-ray diffraction techniques. *Polym. Int.* **2000.** 49(12), 1555-1560.

79. Ries, M.; Pruitt, L. Effect of cross-linking on the microstructure and mechanical properties of ultra-high molecular weight polyethylene. *Lin. Orthop. Relat. Res.* **2005.** 440, 149-156.

80. Zentel, R.; Brehmer, M. Electroactive Liquid Crystalline Polymers. *Polymer Science: A Comprehensive Reference.* **2012.** 8, 129-145.

81. Hildalgo-Ruz et al. Microplastics in the marine environment: a review of the methods used for identification and quantification. *Environ. Sci. Technol.* **2012.** 46, 3060-3975.

82. Strobl, G.; Hagerdorn, W. Raman spectroscopic method for determining the crystallinity of polyethylene. *J. Poym. Sci.: Polym. Phys. Ed.* **1978.** 17, 1181-1193.

83. Zerbi, G. et al. Structural depth profiling in polyethylene films by multiple internal reflection infra-red spectroscopy. *Polymer.* **1989.** 30, 2324-2327.

84. Abbate, S.; Gussoni, M. Infrared and raman intensities of polyethylene and perdeuteropolyethylene: factor group splittings. *J. Chem. Phys.* **1979.** 70, 3577.

85. Chen, Z. The crystallization of poly(ethylene terephthalate) studied by thermal analysis and FTIR spectroscopy. Ph.D. Dissertation, University of Birmingham, Birmingham, UK, 2012.

86. Klute, C. Diffusion of small molecules in semicrystalline polymers: water in polyethylene. *J. App. Polym. Sci.* **1959.** 1, 340-350.

87. Yasuda, H.; Stannett, V. Permeation, solution, and diffusion of water in some high polymers. *Journal of Polymer Science banner.* **1962.** 57(165), 907-923.71

88. Proctor, A.; Toro-Vazquez, J. *Bleaching and Purifying Fats and Oils,* 2nd ed.; AOCS Press: Urbana, IL, 2009.

89. Li, J. Adsorption of anitbiotics on microplastics. *Environ. Pollut.* **2018.** 237, 460-467.

90. Hueffer, T.; Hofmann, T. Sorption of non-polar organic compounds by micro-sized plastic particles in aqueous solution. *Environ. Pollut.* **2016.** 214, 194-201.

91. Bakir, A. et al. Competitve sorption of persistent organic pollutants onto microplastics in the marine environment. *Mar. Pollut. Bull.* **2012.** 64, 2782-2789.

92. Wu, C. et al. Sorption of pharmaceuticals and personal care products to polyethylene debris. *Environ. Sci. Pollut. Res.* **2016.** 23, 8819-8826.

93. United States Environmental Protection Agency. *Guidelines for using passive samplers to monitor organic contaminants at superfund sediment sites.* **2012.** Downloaded Nov. 18, 2018.

94. Saquing, J. et al. Impact of plastics on fate and transport of organic contaminants in landfills. *Environ. Sci. Technol.* **2010.** 44, 6396-6402.

95. Chen, Z.; Hay, J.; Jenkins, M. The thermal analysis of poly(ethylene terephthalate) by FTIR spectroscopy. *Thermochimica Acta.* **2013**. 552, 123-130.

96. Lenz, P.; Lipowsky, R. Morphological transitions of wetting layers on structured surfaces. *Physical Review Letters.* **1998.** 80(9), 1290-1293

97. Brewer, D. Some thermal, magnetic, and flow properties of adsorbed He and He^3-He^4 mixtures. *J. Low. Temp. Phys.* **1970.** 3(3), 204-224.

98. Fisher, M.; Barber, M. Scaling theory for finite-size effects in the critical region. *Phys. Rev. Lett.* **1972.** 28, 1516-1519.

99. Bokria, J.; Schlick, S. Spatial effects in the photodegradation of poly(acrylonitrile-butadiene-styrene): a study by ATR-FTIR. *Polymer.* **2002.** 43(11), 3239-3246.

100. McMurry, H.; Thornton, V. Correlation of infrared spectra: paraffins, olefins, and aromatics with structural groups. *Analytical Chemistry.* **1952.** 24(2), 318-334.

101. Rodriguez-Reinoso, F. *Encyclopedia of Materials: Science and Technology*, 2nd Ed.; Elsevier Lrd.: N/A 2001.

102. Khulbe, K.; Matsuura, T. Removal of heavy metals and pollutants by membrane adsorption techniques. *Applied Water Science.* **2018.** 8(19), np.

103. Fotopoulou, K.; Karapanagioti, H. Surface properties of beached plastic pellets. *Mar. Environ. Res.* **2012.** 81, 70-77.

Appendix

Topic 1: *Fitting crystalline and amorphous peaks on OMNIC from ATR-FTIR*

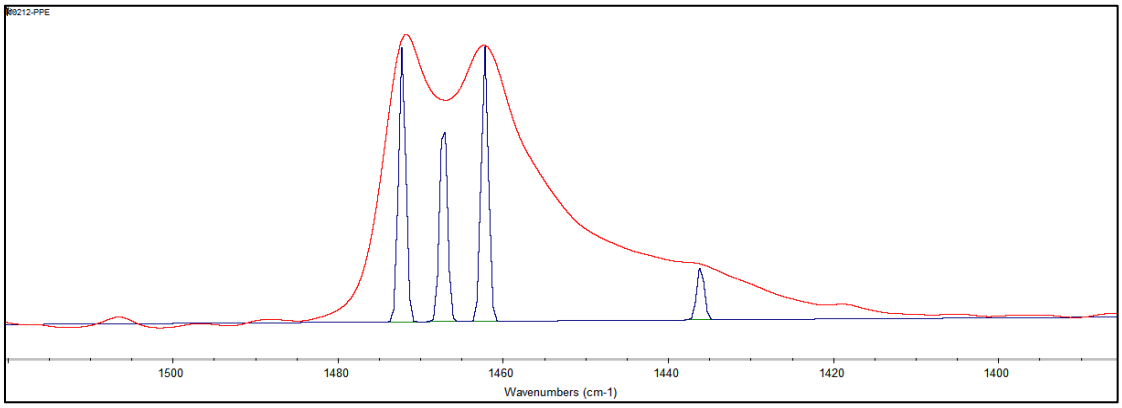

Figure A1.1: After using "Find Peaks" function of OMNIC software.

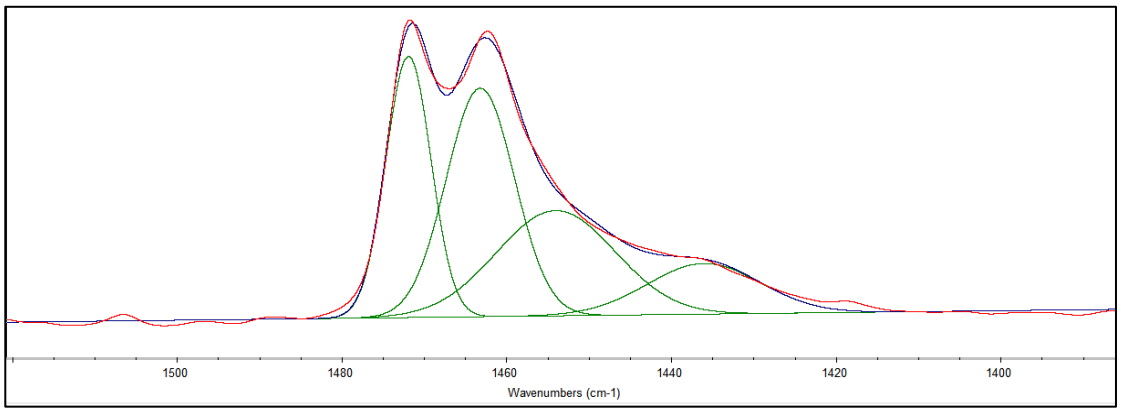

Figure A1.2: After using "Fix Peaks" function of OMNIC software.

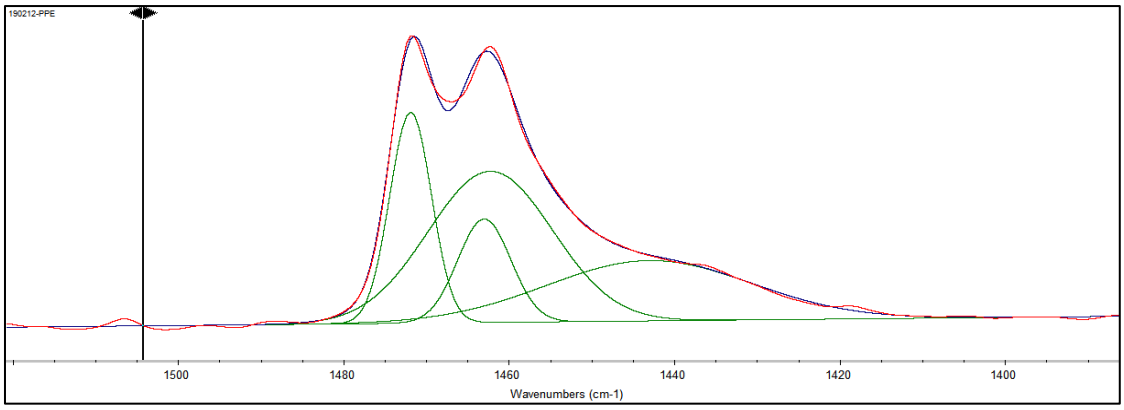

Figure A1.3: After multiple iterations of using "Fix Peaks" function on OMNIC software.

Topic 2: *Adsorption control experiments with glassware and wire.*

Control experiments were conducted by not adding plastic to the sorption vials for the glassware. Once the glassware was determined to not be adsorbing coumarin, the wire control was conducted by placing only the wire mesh, no polymer, in a coumarin solution.

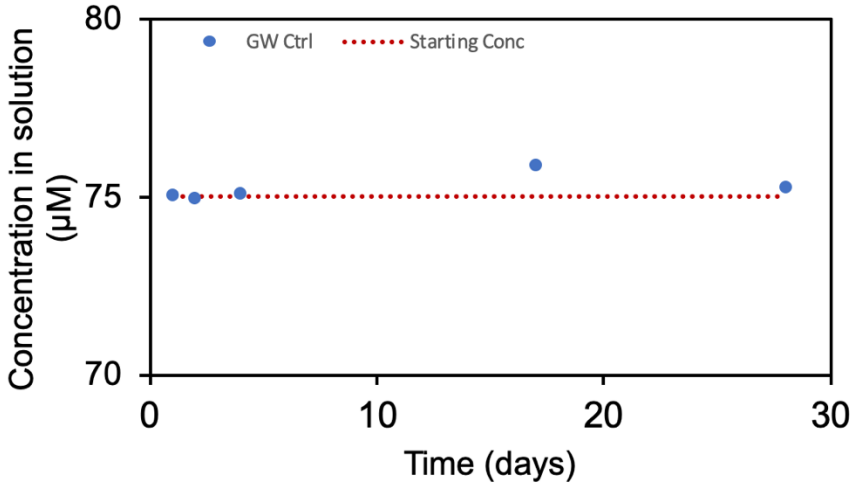

Figure A2.1: Control study of the concentration of Coumarin over time to test adsorption to glass vial. No decrease was observed indicating coumarin is not sorbing to glass.

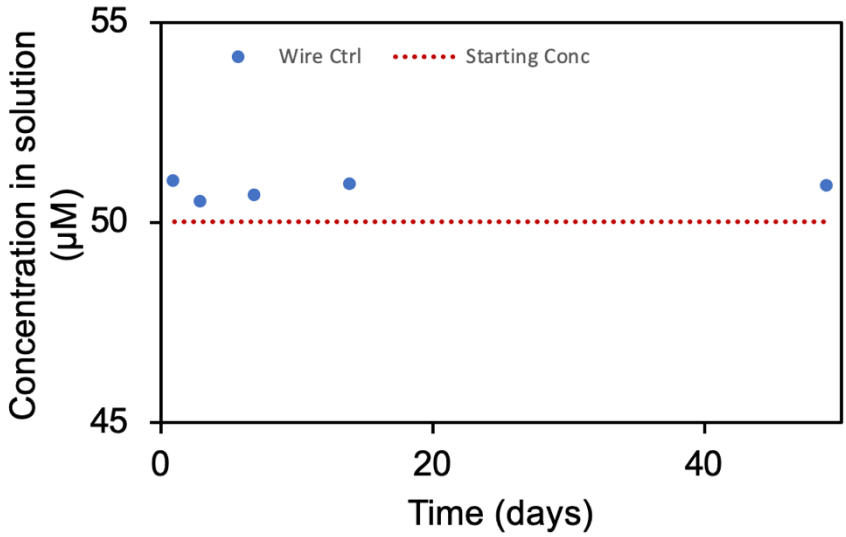

Figure A2.2: Control study of the concentration of Coumarin over time to test adsorption to wire mesh. No decrease was observed indicating coumarin is not sorbing to wire mesh.

Topic 3: *Differential Scanning Calorimetry (DSC) data of PE and PET*

Measurements were performed using a DSC Q 1000 (TA Instruments) on Tzero pans. All sample masses were between 1 and 2.5 mg. A normalization heating cycle from 20℃ to 150℃ for PE and 20℃ to 300℃ for PET was done at a rate of 10℃/minute. This was followed by a cooling cycle, then a second heating cycle.

Processing was performed using TA Instruments Universal Analysis 2000. The second cooling cycle was used for crystallinity measurements. A sigmoidal horizontal baseline was used, and peak area was integrated from ~30℃ to 105℃ for PE and ~90℃ to 210℃ for PET, which represented the onset of changing heat flow until the end of the freezing peak. The integration of the downwards heating peak, with reference to the H_f of 100% crystalline PE and PET (TA Instruments).

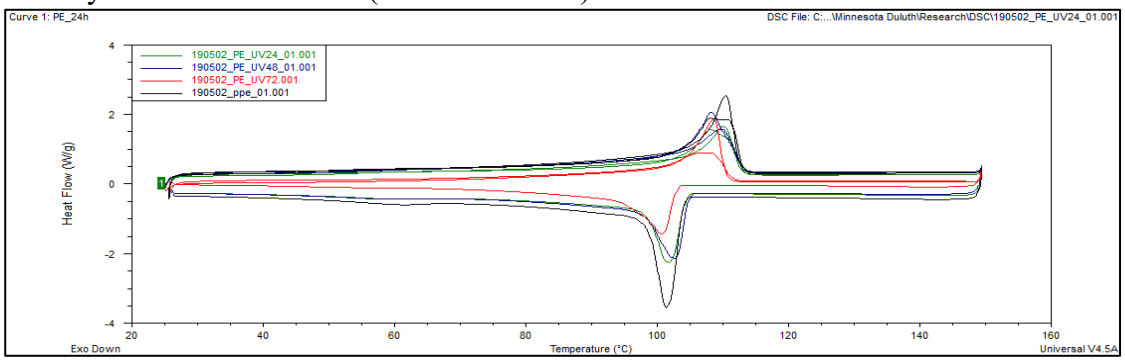

Figure A3.1: Thermogram from DSC runs for PE

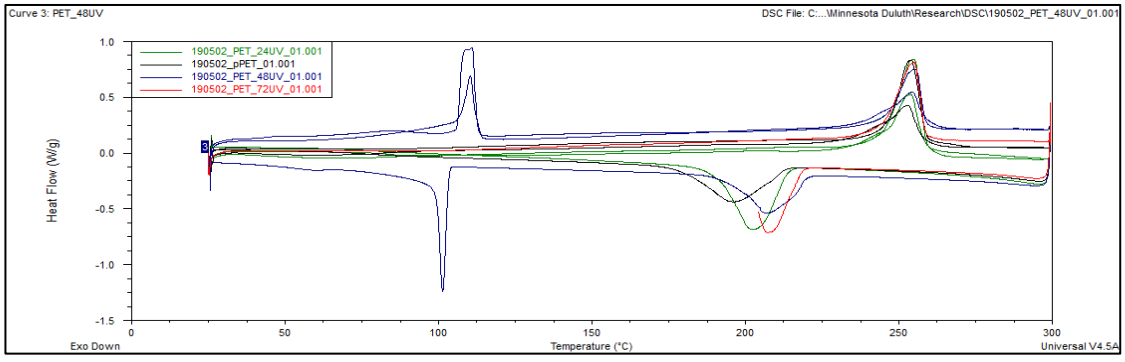

Figure A3.2: Heat curves from DSC runs for PE

Table A2.1. Percent crystallinity values for PE and PET from DSC

Hours Irradiated	PE (%)	PET (%)
0	55.3	60.28
24	39.98	34.94
48	43.20	28.61
72	33.57	N/A

Topic 4: *Chromatograms from HPLC for non- and irradiated PE and PET showing leachates.*

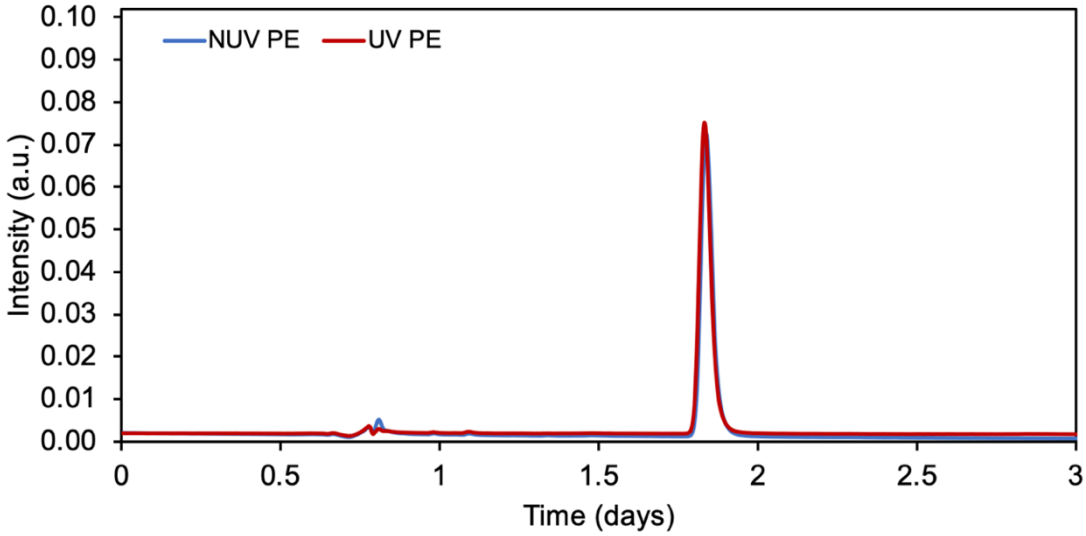

Figure A4.1: Chromatograms for non- and irradiated PE in 10 μM coumarin after 7 days.

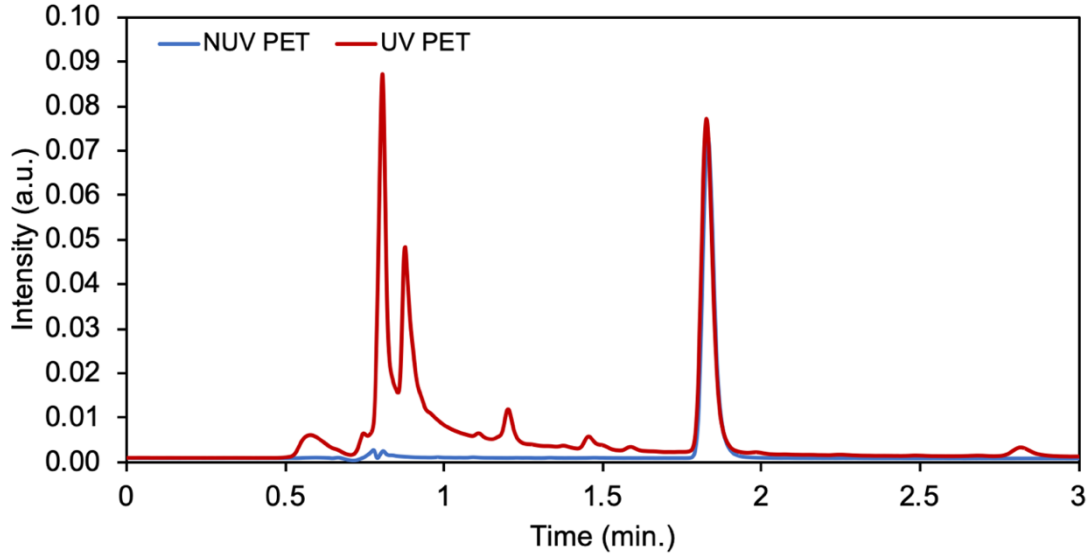

Figure A4.2: Chromatograms for non- and irradiated PET in 10 μM coumarin after 7 days show other small molecules leach from the irradiated films.

Topic 5: *Linearized plots of Langmuir and Freundlich isotherms (Eqn. 3 and 5).*

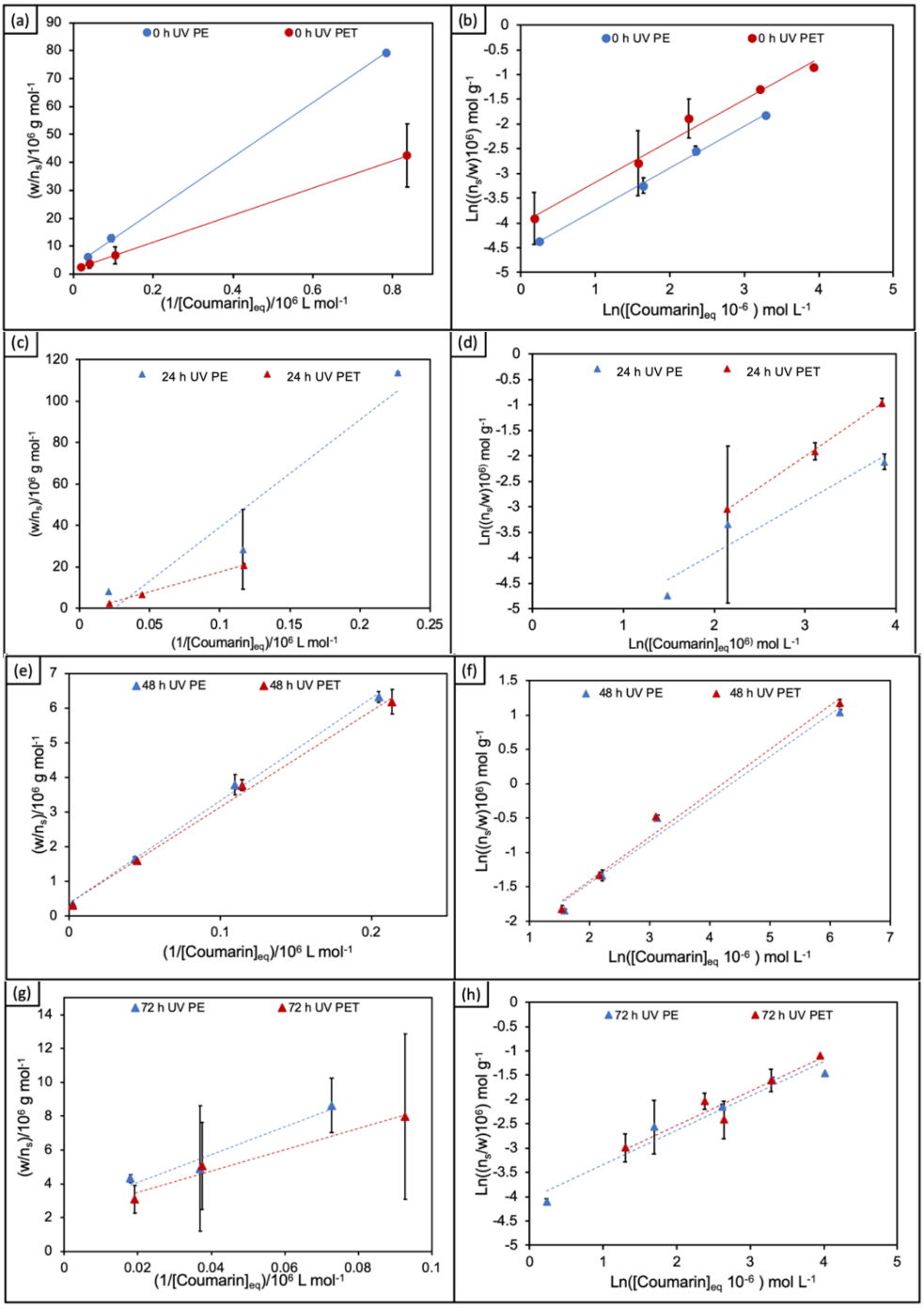

Figure A5.1: (a)Langmuir isotherm and (b) Freundlich isotherm plots for non-irradiated PE and PET. (c)Langmuir isotherm and (d) Freundlich isotherm plots for 24 hour irradiated PE and PET. (e)Langmuir isotherm and (f) Freundlich isotherm plots for 48 hour irradiated PE and PET. (g)Langmuir isotherm and (h) Freundlich isotherm plots for 72 hour irradiated PE and PET.

Topic 6: *Sorption experiments with other model micropollutants.*

1. Ibuprofen: Experiments with ibuprofen did not show sorption but rather an increase in ibuprofen concentration over time. As ibuprofen was the first chemical used, the methodology was not finalized, and nothing was used to prevent evaporation. Also, the carboxylic functional group on the compound may have caused the molecule to ionize and therefore become problematic for chromatographic analysis.
2. Caffeine: Experiments with caffeine brought the addition of parafilm as a way to seal the vials. However, sorption still did not occur. This suggests caffeine was not hydrophobic enough to leave the aqueous phase ($\log K_{ow} = 0.07$).
3. Tetracycline: Tetracycline was only used for a short period of time. It is a chemical that is difficult to work with as it is photosensitive. This created problems as it degraded in solution, so it was decided to not continue working with this chemical.
4. Diuron: This chemical is currently being used. Preliminary data suggests sorption is happening, but only in a 100% aqueous solution. Sorption experiments with a 10% methanol co-solvent showed no sorption.